



**HAL**  
open science

## Oblique rifting triggered by slab tearing: the case of the Alboran rifted margin in the eastern Betics

Marine Larrey, Frédéric Mouthereau, Damien Do Couto, Emmanuel Masini, Anthony Jourdon, Sylvain Calassou, Véronique Miegébielle

### ► To cite this version:

Marine Larrey, Frédéric Mouthereau, Damien Do Couto, Emmanuel Masini, Anthony Jourdon, et al.. Oblique rifting triggered by slab tearing: the case of the Alboran rifted margin in the eastern Betics. Solid Earth, 2023, 14, pp.1221-1244. 10.5194/se-14-1221-2023 . insu-04604310

**HAL Id: insu-04604310**

**<https://insu.hal.science/insu-04604310>**

Submitted on 7 Jun 2024

**HAL** is a multi-disciplinary open access archive for the deposit and dissemination of scientific research documents, whether they are published or not. The documents may come from teaching and research institutions in France or abroad, or from public or private research centers.

L'archive ouverte pluridisciplinaire **HAL**, est destinée au dépôt et à la diffusion de documents scientifiques de niveau recherche, publiés ou non, émanant des établissements d'enseignement et de recherche français ou étrangers, des laboratoires publics ou privés.



Distributed under a Creative Commons Attribution 4.0 International License



# Oblique rifting triggered by slab tearing: the case of the Alboran rifted margin in the eastern Betics

Marine Larrey<sup>1,2</sup>, Frédéric Mouthereau<sup>1</sup>, Damien Do Couto<sup>3</sup>, Emmanuel Masini<sup>4</sup>, Anthony Jourdon<sup>5</sup>, Sylvain Calassou<sup>2</sup>, and Véronique Miegbielle<sup>2</sup>

<sup>1</sup>Université Paul Sabatier, Géosciences Environnement Toulouse, GET UMR 5563, Toulouse, France

<sup>2</sup>TOTAL S.A., Centre Scientifique & Technique Jean Féger, 64000 Pau, France

<sup>3</sup>Sorbonne Université, CNRS-INSU, Institut des Sciences de la Terre Paris, ISTeP UMR 7193, 75005 Paris, France

<sup>4</sup>M&U sas, 38360 Sassenage, France

<sup>5</sup>Institute of Geophysics, Ludwig-Maximilians-Universität München, Munich, Germany

**Correspondence:** Frédéric Mouthereau (frederic.mouthereau@get.omp.eu)

Received: 26 October 2022 – Discussion started: 28 November 2022

Revised: 6 October 2023 – Accepted: 24 October 2023 – Published: 7 December 2023

**Abstract.** The tectonic evolution of highly oblique continental margins that result from extension above lithospheric subduction–transform edge propagator (STEP) faults is poorly understood. Here, we investigate the case of the Alboran margin in the eastern Betics characterized by crustal thinning of 15–10 km, oblique to the direction of slab retreat. The current deformation patterns indicate that oblique rifting is underway. However, it is unclear whether these conditions are those that prevailed during the formation of the metamorphic domes and intramontane basins. We review the temporal and spatial evolution of Neogene sedimentary basins and brittle deformation in the eastern Betics and exploit offshore seismic reflection lines to propose a crustal-scale section across the oblique margin. The history of sediment infill and rates of subsidence combined with the analyses of fault slip data confirm that brittle extension oriented from north 20° E to E–W occurred during an interval spanning from the Serravallian–early Tortonian to the late Tortonian (14–8 Ma). This extension is associated with both normal and strike-slip regimes and the evolution of the strike-slip fault zones flanking the metamorphic domes. The transtensional model forms a coherent scheme linking the ductile deformation associated with metamorphic domes and the formation of E–W- and NW–SE- or NNW–SSE-directed sedimentary basins in the brittle upper crust during the Tortonian. The oblique extension, which is closely associated with STEP faulting, occurred during the regional convergence between

Africa and Iberia since the Miocene. Only recently, around 8 Ma, has slab detachment started to migrate westward, leading to tectonic inversion in the eastern Betics. Such a type of narrow oblique-rifted margin associated with transform-like plate boundaries is not unique but is expected to be hardly preserved in the geological record due to the transient nature of retreating subduction systems.

## 1 Introduction

### 1.1 Tear faulting and oblique crustal thinning in the Betics

Lithospheric tear faults or subduction–transform edge propagator (STEP) faults are propagating strike-slip faults that accommodate the differential motion between the retreating subduction zone and the overriding plate (Govers and Wortel, 2005). Because of the relative motion between back-arc and surrounding plates, they are also propagating strike-slip faults defined by a sharp contrast in crustal thickness. As noted by Govers and Wortel (2005), such oblique fault boundaries do not necessarily form proper transform plate boundaries, but instead form broad zones of distributed deformation, accommodating differential trench-parallel extension, strike-slip motion, and rotation. In case the lithospheric tear propagates within the continent–ocean transition, a nar-

row continental margin forms highly oblique to the direction of back-arc extension. This is documented, for instance, in the Caribbean, along the transcurrent Caribbean–South American plate boundary (Pindell and Kennan, 2009) or on the margin of the South Orkney Microcontinent, along the Scotia–Antarctic plate boundary (Dalziel et al., 2013). Despite the large-scale kinematic picture being relatively well understood, there are only a few places on Earth where continental crustal deformation associated with a slab edge continental rift system can be studied both on land and offshore.

Here, we focus on the eastern Betic Cordillera, which constitutes a rifted margin defined by decreasing crustal thickness from  $> 35$  to 20 km onshore (Diaz et al., 2016), thinning offshore to 16–6 km in the eastern Alboran arc to the back-arc region (Booth-Rea et al., 2018; Gómez de la Peña, 2020a) (Figs. 1 and 2). This region is seen to develop above a E–W-trending STEP fault at the boundary between the Alboran basin and the Iberian paleomargin (Badji et al., 2014; Galais et al., 2013; Jolivet et al., 2021a; Mancilla et al., 2015a). The tectonic expression of the strike-slip deformation during E–W-directed crustal extension above the lithospheric tear is, however, controversial. On the one hand, low-angle ductile extensional detachments with a top-to-the-west sense of shear are the main features accommodating deformation in the overriding plate. Yet, A-type metamorphic domes in the lower crust, elongated parallel to the E–W direction (Fig. 1) and formed during the early Miocene, are viewed to express the transtensional deformation at the tip of propagating tear (Le Pourhiet et al., 2012). On the other hand, E–W-directed transfer strike-slip faulting is interpreted as a late (post-middle Miocene) brittle deformation feature associated with differential E–W crustal extension between the metamorphic domes in the eastern Betics (Alpujarras fault zone; Sanz de Galdeano and Vera, 1992; Sanz de Galdeano et al., 1985; Martínez-Martínez et al., 2006) and in the western Betics (Torcal fault zone; Barcos et al., 2015) unrelated to ductile deformation (Fig. 1). In line with the latter interpretation, the dextral motion these transfer faults accommodate is assumed to be modest, reflecting a recent post-8 Ma kinematic change that accompanies the stalling of westward slab rollback, the onset of tectonic inversion in the Gibraltar Arc (Do Couto et al., 2014; d’Acremont et al., 2020; Jolivet et al., 2021a; Martínez-García et al., 2017), and progressive slab tearing and delamination of the lithospheric mantle from the eastern to the central Betics (Martínez-Martínez et al., 2006; Mancilla et al., 2015a; García-Castellanos and Villaseñor, 2012; Spakman et al., 2018). Note that in a recent study the dextral displacement since 9 Ma has been estimated to more than 100 km along the Torcal Fault (Crespo-Blanc et al., 2016).

The lack of structural temporal constraints and quantification of belt-parallel motion along these faults indicates, however, that we do not yet fully understand their link with the long-term evolution of slab tearing and margin formation. For instance, the current deformation patterns in the central Betics, where metamorphic domes are present, brings evi-

dence that both strike-slip faulting and extension operate synchronously (Martínez-Martínez et al., 2006). This is shown by the west-directed GPS velocities increasing westwards indicating ongoing extension, and the west-directed displacements increasing from north to south, towards the Alboran domain, revealing right-lateral shear (Fig. 2). This, together with evidence for present-day  $4.5 \text{ mm yr}^{-1}$  westward displacement and rotations in the western Betics and Rif, reveals that the westward slab rollback is likely to be still ongoing (Fadil et al., 2006; Gonzalez-Castillo et al., 2015). The current transtensional deformation across the Betic Cordillera is consistent with the current stress regime defined by extension direction highly oblique (max.  $20^\circ$ ) to the Betic structural trend (or  $70^\circ$  spanned by the direction of extension and normal of the rift trend).

## 1.2 Highly oblique rifting triggered by slab tearing: a proof of concept in the eastern Betics

Right-lateral transtensional deformation in the Betics agrees with the extrusion model of the Alboran basin towards the Gibraltar Arc to the west (Borque et al., 2019; Palano et al., 2015) caused by indentation by the east Alboran domain likely enhanced by resistance slab dragging (Spakman et al., 2018). In the east, the extrusion is accommodated by left-lateral strike-slip displacement along the Eastern Betic Shear Zone (EBSZ; Borque et al., 2019), shaped by the Carboneras Fault (CF) and Palomares Fault (PF), which separates the extrusion domain, where extension and transtension is prevailing, from the Águilas Arc, where N–S indentation is well documented (Ercilla et al., 2022). In this region, this fault extends offshore, across the Alboran Sea, in the larger Trans-Alboran Shear Zone (De Larouzière et al., 1988; Stich et al., 2006) moving at  $\sim 4 \text{ mm yr}^{-1}$ , equivalent to the regional  $5 \text{ mm yr}^{-1}$  NW-directed convergence between Africa (Nubia) and Europe (Fig. 2; Echeverría et al., 2013; Koulali et al., 2011; Nocquet, 2012; Palano et al., 2015, 2013; Vernant et al., 2010). Here, we hypothesize that the present-day oblique extension pattern has been at play since the Miocene and explains the formation of the narrow Alboran rifted margin.

Only recently high-resolution 3D numerical models have been able to predict the deep structure of oblique rift domains. These models can be used as a guide to re-evaluate the evolution of the Betics. Three-dimensional models by Jourdon et al. (2021) predict that oblique extension results in narrow rifted margins, strike-slip faults, and corridors coupled with subsident pull-apart basins, normal faults, and block rotations (Fig. 3). The recognition of block rotation in the Betic Arc (Crespo-Blanc et al., 2016; Platzman, 1992), strike-slip fault zones (Fig. 1) and NW–SE normal faulting, which defines extension direction highly oblique to the margin (Galindo-Zaldívar et al., 2003; Figs. 1 and 2), support this view. The simulations also show that the deeper ductile crust experiences thinning (vertical flattening) and stretching

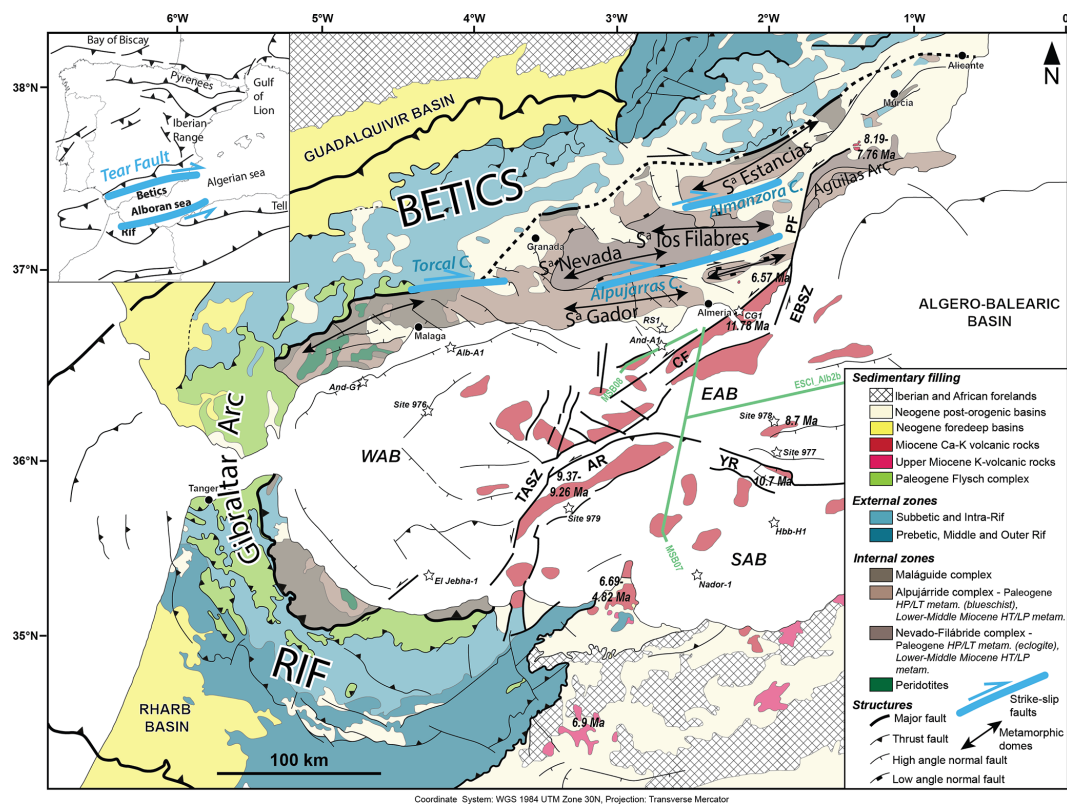


**Figure 1.** Geological map of the Betic–Rif arc. Main tectonic units and the age of volcanism, as well as major structures and Neogene sedimentary basins, are shown. The studied offshore seismic lines (red) and offshore wells and ODP sites (open star) for stratigraphic calibration in the eastern (EAB), southern (SAB), and western Alboran basins (WAB) are displayed. CF stands for Carboneras Fault, PF stands for Palomares Fault, AR stands for Alboran Ridge, YR stands for Yusuf Ridge, EBSZ stands for East Betic Shear Zone, and TASZ stands for Trans-Alboran Shear Zone.

perpendicular to the strike of the margin in accordance with stretching lineations parallel to the metamorphic domes and low-angle detachments (Fig. 3). Other types of 3D numerical experiments show that sediment loading of strike-slip faults can result in asymmetric flexural basins with apparent normal fault throw (Neuharth et al., 2021) that can be mistakenly interpreted as resulting from orthogonal extension. Asymmetric basins are indeed intriguing characteristics of intramontane basins in the Betics (Rodríguez-Fernández et al., 2012; Augier et al., 2013; Do Couto et al., 2014; Giaconia et al., 2014). Although primarily found associated with divergent plate boundaries, e.g. in the Gulf of California (Fossen et al., 2013; Fossen and Tikoff, 1998), highly oblique extension is also documented in active transform regions along the San Andreas Fault (Teyssier and Tikoff, 1998) or the North Anatolian Fault in the Sea of Marmara (Okay et al., 2004). A detailed analysis of highly oblique rifting deformation in the Gulf of California recognizes similar tectonic elements to those for the Betics, such as extensional detachment systems orthogonal to the divergence and upper crustal folds trending parallel to the divergence (Fossen et al., 2013).

However, several tectonic features need further discussion. First, the relevance of strike-slip faulting in the past is debatable as only a few occurrences of crustal-scale strike-slip faults are mapped (Fig. 1). Second, the detail of the temporal and spatial relationships between the formation of the oblique–transform margin and STEP faulting remain elusive. We here review the temporal and spatial evolution of Neogene intramontane sedimentary basins and related brittle deformation in the eastern Betics. In addition, we exploit offshore seismic reflection lines to propose a new crustal-scale section across the oblique margin. Based on these constraints we present a tectonic scenario for the formation of the high-obliquity rifted margin controlled by STEP faulting.

## 2 Geodynamics and STEP faulting in the Betics

The onset of N-directed movement of Africa, by the Late Cretaceous–Paleogene, led to far-field, Laramide-like contraction from Morocco throughout western Europe (Mouthereau et al., 2021). South of Iberia, in the Betic–Rif domain, the closure of hyper-extended rift systems and oceanic basins of the Atlantic–Alpine Tethys resulted in

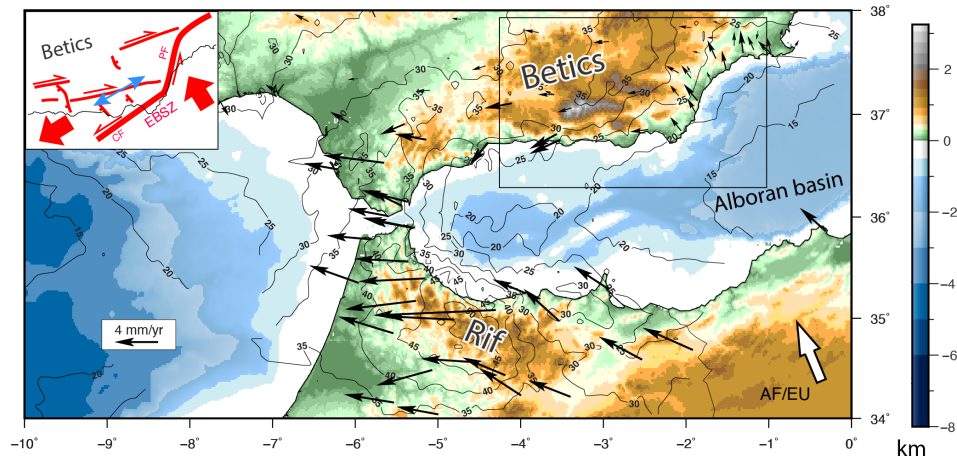


**Figure 2.** Present-day kinematics in the Betic–Rif Arc and eastern Betic Cordillera (inset). GNSS-based displacements in the western Alboran block and northwestern Africa shown in a fixed Eurasian reference frame (black arrows after Palano et al., 2015) are oblique to the African–European plate convergence (white arrow) inferred from plate tectonic Morvel model (Argus et al., 2011). Labelled contours depict the crustal depth given in kilometres as inferred from deep seismic profiles and receiver function analysis (Diaz et al., 2016). In the eastern Betic (inset), W-directed stretching is taken up by an E–W-directed right-lateral strike-slip fault and NW–SE normal faults. Extension direction resolved from focal mechanisms (blue arrow) are after Stich et al. (2006). CF stands for Carboneras Fault, PF stands for Palomares Fault, AR stands for Alboran Ridge, YR stands for Yusuf Ridge, EBSZ stands for East Betic Shear Zone, and TASZ stands for Trans-Alboran Shear Zone.

the development of a proto-Betic accretionary prism, likely largely submerged (Angrand and Mouthereau, 2021; Daudet et al., 2020; Vergés and Fernández, 2012). By about 50 Ma, the acceleration of plate convergence led to the shortening of continental rift and oceanic basins and topographic uplift all over Iberia (Daudet et al., 2020; Mouthereau et al., 2021, 2014; Rat et al., 2019; Vacherat et al., 2016; Waldner et al., 2021) associated with the onset of continental rifting along the western European Rift (e.g. Mouthereau et al., 2021). At 35 Ma, as African convergence slowed down, the western Mediterranean Sea opened, accompanied by retreating slabs (Dewey, 1988; Dewey et al., 1989; Faccenna et al., 2014; Jolivet and Faccenna, 2000; Rosenbaum et al., 2002). Subduction occurred mainly before 30 Ma, as argued by age constraints on high-pressure mineral assemblages (Augier et al., 2005a; Bessière et al., 2021; Booth-Rea et al., 2015; Gomez-Pugnaire and Fernandez-Soler, 1987; Platt and Visser, 1989; Platt and Whitehouse, 1999) and has been suggested to last until the mid-Miocene in the eastern Betics (e.g. Platt et al., 2013). The timing of formation of the Alboran basin is constrained to 23 to 16 Ma by the oldest deposits found on Alboran basement and by the timing of high-temperature metamorphic overprint and rapid cooling to shallow crustal temperature (Bessière et al., 2021; Daudet et al., 2020; Janowski et al., 2017; Johnson et al., 1997; Platt et al., 2005; Sosson et al., 1998; Vázquez et al., 2011; Zeck et al., 1992). The eastern Alboran basin formed later, mostly by late Miocene arc magmatism (Booth-Rea et al., 2007, 2018; Gómez de la Peña et al., 2020a).

All kinematic reconstructions agree that extension results from the westward migration of the arc front and retreat of the Alboran slab, well imaged below the Gibraltar Arc as a steeply dipping high-velocity anomaly (Bezada et al., 2013; Heit et al., 2017; Mancilla et al., 2018, 2015a, b; Palomeras et al., 2014; Spakman and Wortel, 2004; Villaseñor et al., 2015). These reconstructions, however, differ according to the paleo-position of Alboran terrane, and hence in the amount and vergence of subduction (Angrand and Mouthereau, 2021; van Hinsbergen et al., 2014; Lonergan and White, 1997; Romagny et al., 2020; Rosenbaum et al., 2002; Vergés and Fernández, 2012). Seismic tomography reveals that slab detachment and tearing occur along the conjugate Alboran margins of the southern Betics and northern Africa (Govers and Wortel, 2005; Heit et al., 2017; Mancilla et al., 2015a; Meighan et al., 2013; Spakman and Wortel, 2004).

In Fig. 4 we refer to the reconstruction of Angrand and Mouthereau (2021) that has the advantage of reconciling previous western Mediterranean models (Romagny et al., 2020; Vergés and Fernández, 2012) with recent thermochronological analyses in western Betics (Daudet et al., 2020) and other geological data (see compilation in Mouthereau et al., 2021). This model considers that the Alboran domain has been rifted from Iberia during the Jurassic. It is in agreement with detrital and igneous zircon U–Pb ages that suggest Alboran was attached to Iberia in the late Paleozoic (Jabaloy-Sánchez et al., 2021). It also accounts for the existence of an upper Cretaceous–Paleogene foreland basin that formed adjacent to a proto-Betic orogen and in continuity eastwards with

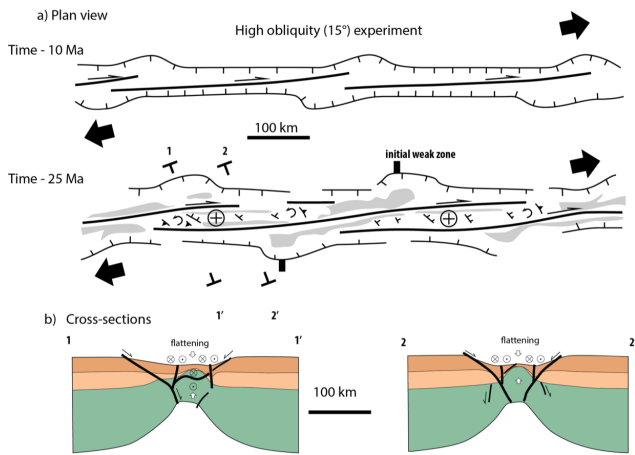


**Figure 3.** Sketch of highly oblique rift experiments based on the results of a 3D thermo-mechanical model (Jourdon et al., 2021). Results are depicted in plan view (a) and cross sections (b) for two steps (after 10 and 24 Myr) for the case where extension is set with an angle of  $15^\circ$  with respect to the rift axis. Grey regions in (a) are basins adjacent to uplifted domains (cross-circle symbol) associated with right-lateral strike-slip faults. Cross-sections (b) depict the abrupt crustal thinning that occur perpendicularly. Crustal thinning is most visible for the lower crust and produces the formation of an abrupt necking domain controlled by rift-parallel normal faults dipping towards the centre of the rift and right-lateral strike-slip faults.

the Balearic Promontory. In that respect, it contrasts with other models placing the Alboran domain to the south of the Balearic Promontory (Moragues et al., 2021; van Hinsbergen et al., 2014).

In this reconstruction about 400 km of slab retreat is estimated since about 35 Ma (grey path, blue arrows in Fig. 4). It is worth noting that for Romagny et al. (2020) a similar amount (i.e. 400 km) is accommodated by back-arc extension of the Alboran crust, implying the same magnitude of displacement along the STEP fault in the Betics. In the reconstruction of Angrand and Mouthereau (2021), however, crustal thinning in Alboran basin is linked to delamination retreat of the Alboran lithospheric mantle towards the west. Because of the decoupling between crust and mantle, the length of the delaminated slab resolved at depth in seismic tomography should not be simply translated into the amount of E–W crustal extension in the Alboran domain. This further implies that the displacement across the STEP fault must be also less than 400 km. Daudet et al. (2020) suggested that an extension of 110 km estimated from the restoration of low-angle detachment systems in the central and eastern Betics (Martínez-Martínez et al., 2002) is likely to be a more accurate crustal estimate of the movement Alboran domain rather than the total slab length.

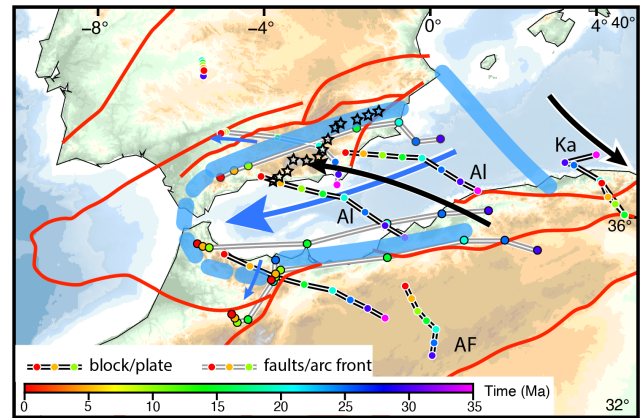


**Figure 4.** Kinematics of the African plate (AF) and Alboran (Al) and Kabylides (Ka) blocks with respect to fixed European plate since 35 Ma reconstructed after Angrand and Mouthereau (2021). Thick blue lines depict the approximate position of lithospheric tear faults (between Al and Europe and Africa) and transfer faults (between Al and Ka). Tear faults located in Betics and Rif are after Jolivet et al. (2021b). Black stars depict the positioned of the tear fault in the Betics as defined by Mancilla et al. (2015a). Black arrows indicate the movement of Al and Ka with respect to Europe along black motion paths presented from 35 Ma to present. Grey motion paths refer to the motion of specific structures relative to Europe, including the motion of the arc front (thick dashed blue line) and faults in red. The dark blue arrows depict the movement of the arc front due to retreating delamination towards the west.

### 3 Miocene extension in the eastern Betics

#### 3.1 Relationships between domes and basins: from transtension and pure extension to late tectonic inversion

The most prominent extensional features in the eastern Betics are (1) the E–W elongated ranges that formed metamorphic domes with foliations bearing prominent E–W stretching lineations, for instance, in the Nevado-Filábride Complex (Fig. 5; e.g. Sierra de los Filabres, Sierra Nevada, and the Sierra de las Estancias) and Serravallian-Tortonian sedimentary basins (Tabernas-Sorbas, Alpujarras, Almanzora and Huércal-Overa basins), and (2) the NNW–SSE and NW–SE normal fault systems and basins oblique to the domes such as the NW–SE-trending Guadix-Baza and Alhabia basins (Galindo-Zaldivar et al., 2003; Martínez-Martínez and Azañón, 1997) (Fig. 5). They are described as asymmetric half grabens (Do Couto et al., 2014; Martínez-Martos et al., 2017; Pedrera et al., 2010, 2009) formed during the upper Serravallian–early Tortonian (Augier et al., 2005b, 2013; Meijninger and Vissers, 2006). Several of these NW–SE faults are active and cut across the metamorphic domes and the sedimentary basins (Augier et al., 2005a; Booth-Rea et al., 2004a; Giaconia et al., 2012; Montenat and d’Estevou, 1999).

In addition to these structures, there are E–W right-lateral strike-slip fault zones and parallel depressions, like the Alpujarras fault zone between the Sierra de Gádor and the Sierra Nevada and the Almanzora fault zone between the Sierra de los Filabres and Sierra de las Estancias (Fig. 5). The left-lateral Carboneras and Palomares fault system (Reicherter and Hübscher, 2006; Scotney et al., 2000) marks the tectonic limit with the Cabo de Gata volcanic province (Fig. 5).

The domes are extension-related features interpreted either as (1) E–W metamorphic domes resulting from the exhumation in the footwall of a regional W-directed extensional low-angle detachments, later folded during post-Tortonian N–S contraction (Martínez-Martínez and Azañón, 1997; Martínez-Martínez et al., 2002, 2004) or (2) Miocene metamorphic domes formed by constrictional ductile strain regime accompanying W-directed stretching of the Alboran domain and trench retreat, with limited overprint by the Tortonian contraction ca. 8 Ma (Augier et al., 2013, 2005c b; Galindo-Zaldivar et al., 2015; Jolivet et al., 2021b; Martínez-Martínez et al., 2002). Low-temperature constraints from the Nevado-Filábride and Alpujarride complexes confirm the W-directed exhumation of the basement that occurred progressively from the Sierra de los Filabres at ~13–11 Ma (Serravallian) in the east to the Sierra Nevada at 8–6 Ma (Late Tortonian–Messinian) in the west (Clark and Dempster, 2009; Janowski et al., 2017; Johnson et al., 1997; Platt et al., 2005; Reinhardt et al., 2007; Vázquez et al., 2011).

Tectonic models for the formation of Neogene intramontane sedimentary basins vary depending on the prevailing tectonic regime. E–W-directed basins have been early described as pull-apart basins (e.g. Alpujarras fault zone; Sanz de Galdeano et al., 1985). Structural analyses then led to reinterpret these structures as transfer zones resulting from differential extension between exhuming core complexes (and detachment systems) since the Serravallian (13–11 Ma) later refolded during Tortonian (9–8 Ma) compression in the eastern Betics while extension is still active in the central Betics (Martínez-Martínez et al., 2006). Other authors proposed that NE–SW extension lasted until 7.5–7 Ma in the eastern Betics (Booth-Rea et al., 2004b; Giaconia et al., 2014).

In support to the compressional stress regime in the eastern Betics, Martínez-Martos et al. (2017) interpreted the E–W depressions as being related to the tectonic reactivation of crustal weakness zone as dextral strike-slip faults in an anticlockwise rotation, accommodating part of the N–S shortening. There is evidence that at the end of the Tortonian a regional uplift occurred, raising the remnants of late Tortonian marine platform, 7.2 Ma in age, to 1600 m above sea level in the Sierra de Gádor (Braga et al., 2003; Janowski et al., 2017), coincidentally with the onset of contraction in the Sierra Alhamilla and Sierra de los Filabres (e.g. Do Couto et al., 2014), in the Alboran domain (e.g. Martínez-García et al., 2017), and on the margins of the eastern Betic (Giaconia et al., 2013, 2015). In addition to shortening, this recent uplift may reflect deep-mantle mechanisms like slab tearing or

delamination (e.g. Duggen et al., 2003; García-Castellanos and Villaseñor, 2012; Mancilla et al., 2015a).

Based on the prevalence in some E–W-trending basins, like the Huércal-Overa basin, of E–W-trending normal faults, these basins have alternatively been interpreted as resulting from late exhumation stage of the domes, possibly as soon as the Serravallian but mostly after the early Tortonian (syn-sedimentary faulting) (Augier et al., 2013, 2005b; Meijninger and Vissers, 2006). The NW–SE or NNW–SSE sedimentary basins (Guadix, Baza, Alhabia; Fig. 5), in contrast, are extensional basins formed parallel to the direction of the regional compression (Sanz de Galdeano and Vera, 1992; De Larouzière et al., 1988). E–W strike-slip fault zones, aligned in the direction of the domes, and NW–SE normal faulting patterns are both key features consistent with predictions from models of oblique extension at transform margin (Fig. 3). Yet, based on existing structural and tectonic syntheses a clear temporal relationship between E–W ductile stretching in the domes and transcurrent deformation is not established (Fig. 5).

### 3.2 Is the Tortonian rift-related subsidence consistent with oblique extension?

The stratigraphic architecture and depositional evolution of Tortonian intramontane basins provides first-order information on the distribution of crustal thinning. Among the oldest sediments deposited unconformably on the Paleozoic–Triassic basement are the red alluvial conglomerates and deltaic series dated from the Serravallian to the Lower Tortonian (Fig. 6a). They are thicker and well exposed on the flanks of the Almanzora basin and on the northern Huércal-Overa basin (HOB), compared to the Alpujarras Corridor (AC) and Tabernas basin (TB) (Figs. 6 and 7a; Augier et al., 2013; Pedrera et al., 2010, 2007; Poisson et al., 1996). In the east of the Sorbas basin, it should be noted that Langhian–Serravallian deposits and perhaps sediments as old as Burdigalian have been locally reported (Giaconia et al., 2014).

Paleogeographic reconstructions indicate that these Serravallian to Lower Tortonian sediments were deposited on a large emerged domain, stretching from Huércal-Overa to Granada in the west and Tabernas to the south (Braga et al., 2003). Sourced from the Nevado-Filábride metamorphic complex (Hodgson and Haughton, 2004; Kleverlaan, 1989; Meijninger and Vissers, 2006; Pedrera et al., 2010, 2007; Pickering et al., 2001; Weijermars et al., 1985), these deposits mark the onset of surface exhumation of the Sierra de las Estancias and Sierra de los Filabres.

During this initial stage, HOB is the most subsident basin (Figs. 6b, 7a, b), accumulating sediments at rates of 400 m Myr<sup>-1</sup> while rates are 140–180 m Myr<sup>-1</sup> in the Tabernas basin (Fig. 6b) (Augier, 2004). Higher subsidence in the HOB, which also started earlier than in other basins, suggests extension occurred originally to the north associated with the exhumation of the Sierra de Las Estancias. Basal continental conglomerates are overlain by grey coarse-grained Tortonian

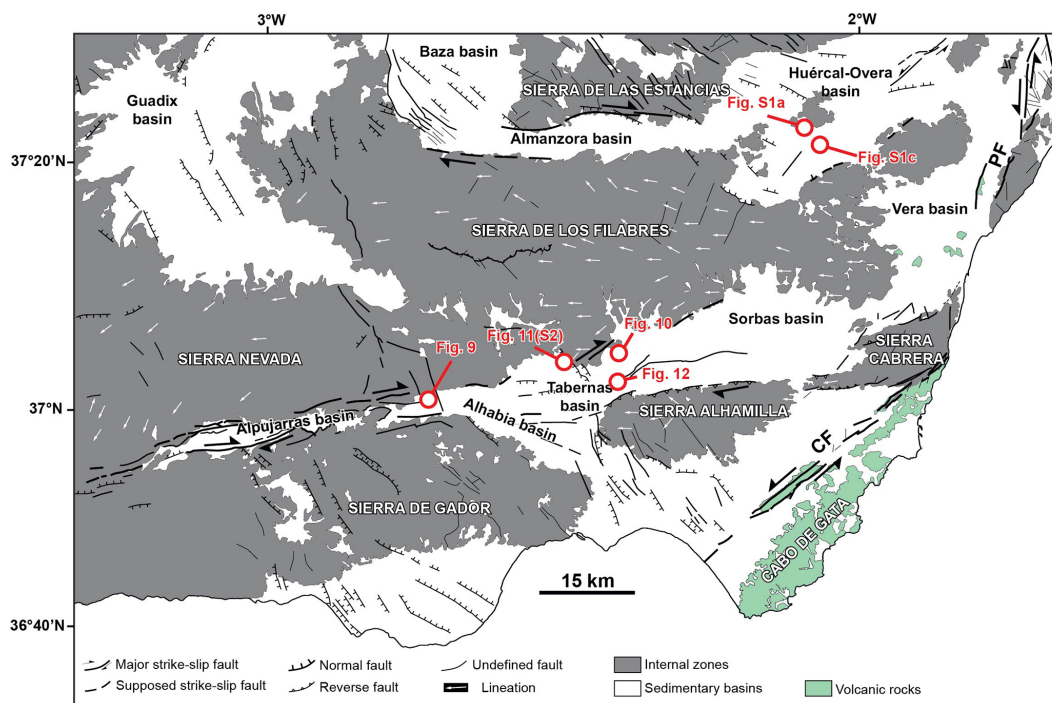


**Figure 5.** Tectonic map of the eastern Betics showing the main structural elements in black after Augier et al. (2005) and Do Couto (2014). CF stands for Carboneras Fault. PF stands for Palomares Fault.

sandstones found occasionally, e.g. in the Almanzora basin, intercalated with marine marls (Fig. 6a). They are topped by mid-Tortonian bioclastic calcarenite and coral reefs (Braga et al., 2003; Martin et al., 1989; Pedrera et al., 2007).

During the same interval, TB recorded the deposition of 300 to 400 m of coarse- to medium-grained deltaic marine clastics unconformably overlying the lowermost red series (Fig. 6a). These sediments pass upwards, e.g. in TB, to deeper marine 1200 m thick turbiditic and marls series intercalated with regional-scale mega-beds, revealing the onset of rapid tectonic subsidence (Haughton, 1994; Kleverlaan, 1989, 1987; Pickering et al., 2001; Weijermars et al., 1985). Details of depositional architecture of the Tortonian suggest that part of this subsidence evolution was controlled by E–W dextral strike-slip faults (Haughton, 2000; Baudouy et al., 2021) under transtensional strain.

The transition from continental to deep marine sedimentary environments (water depth of 400–600 m according to Poisson et al., 1999) witnesses the rapid rift-related tectonic subsidence achieved during the upper Tortonian times ( $\sim 9$  Ma; Figs. 6 and 7c) (Augier et al., 2005b; Montecat and Ott d’Estevou, 1992; Weijermars et al., 1985). At around 8 Ma, accumulation rates drop by a factor of two to  $200 \text{ m Myr}^{-1}$  in HOB and  $70 \text{ m Myr}^{-1}$  in TB, revealing a marked reduction in subsidence. Subsidence then became negative as basement uplifted from around 7 Ma (Figs. 6b and 7d) in both TB and HOB.

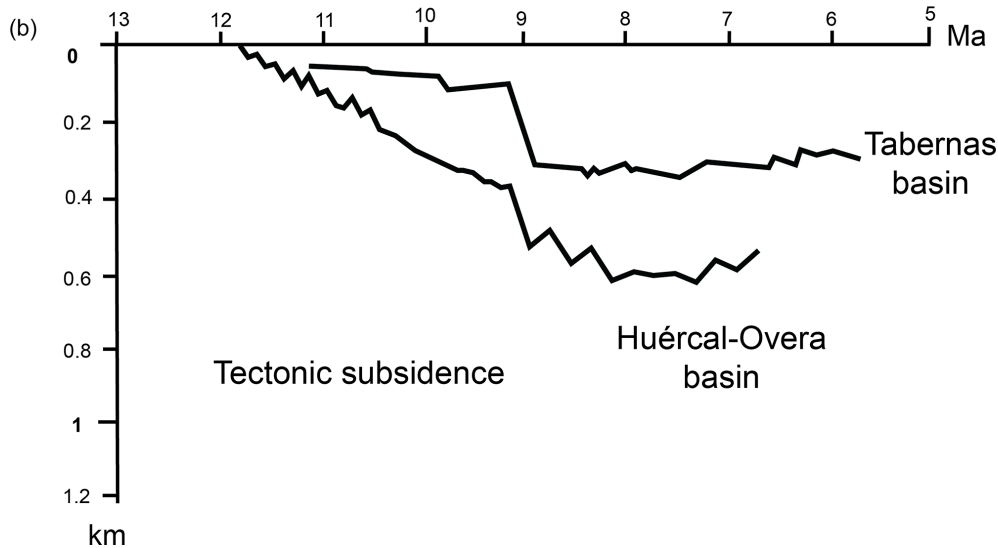
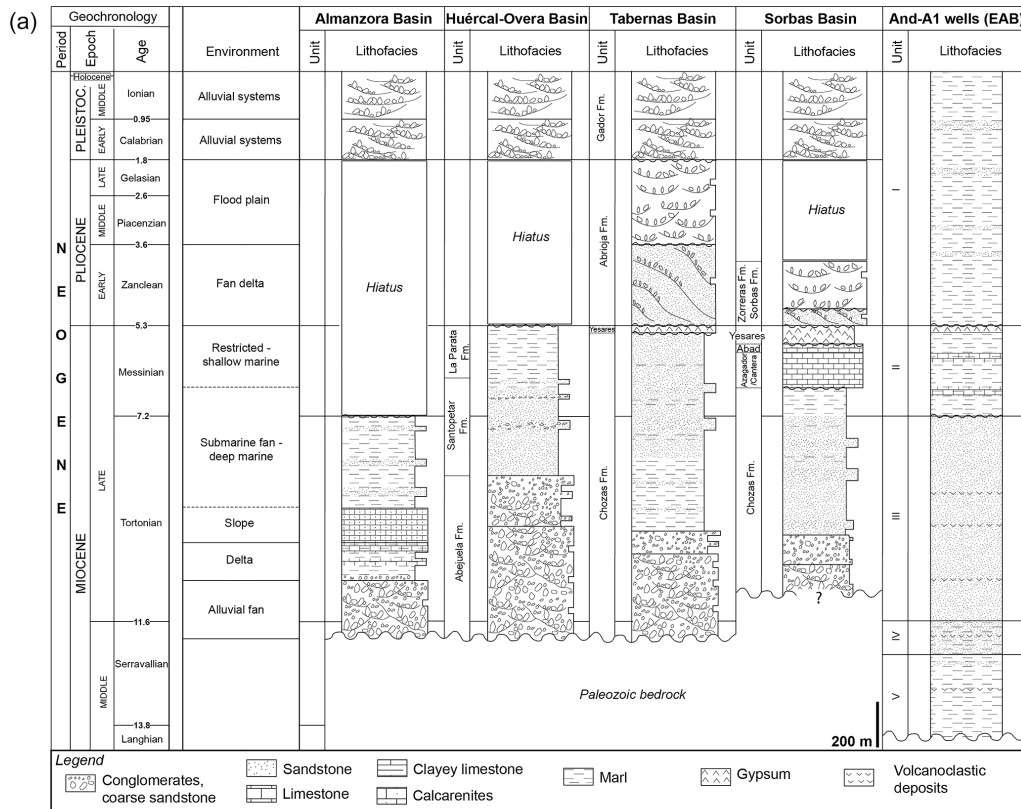
The geometry of the Almanzora (Pedrera et al., 2009), Sorbas (e.g. Do Couto et al., 2014) and Huércal-Overa basins (Pedrera et al., 2010) inferred from gravity measurements indicate that these basins are asymmetrical and deepening southwards. This sediment infill pattern recalls the formation of asymmetrical basins predicted by numerical models of flexural strike-slip basins (Neuharth et al., 2021). According to this model, the asymmetry observed should reflect the development of strike-slip basins loaded by sediments originating from the north. In addition, a larger subsidence in HOB is an indication of abrupt crustal thinning to the south of Sierra de las Estancias where the crustal thickness is the largest (Fig. 2). Therefore, at least the Serravallian–Tortonian infill patterns agree with oblique extension.

#### 4 Brittle faulting: pure extension versus transtensional deformation in Neogene basins

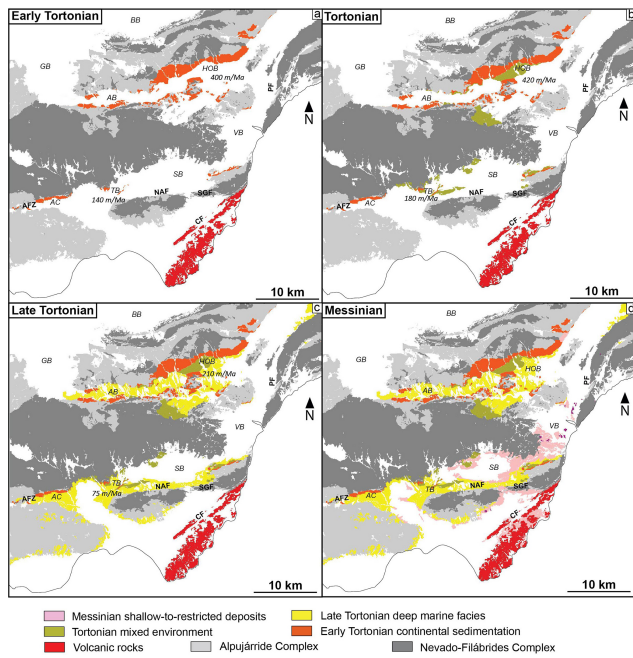
##### 4.1 Tectonic regime in the eastern Betics

Figure 8 presents a compilation of 112 fault slip data inversions previously analysed in the eastern Betics combined with new measurements conducted in the Alpujarras Corridor and in the Tabernas basin (Table S1 in the Supplement). Most faults are syn-Tortonian or cut through the Tortonian. This compilation emphasizes a regional trend of  $\sigma_3$  stress axes oriented NNE–SSW (north  $0^\circ$  E) with subordinate  $\sigma_3$  oriented E–W. In detail, this well-defined regional horizon-





**Figure 6.** Stratigraphic evolution and lithologies of intramontane basins in the eastern Betics and the offshore A1 well. **(a)** Neogene stratigraphy and basin-fill correlation in the Almanzora and Huércal-Overa basins (Mora, 1993), Tabernas basin (Hodgson and Haughton, 2004; Kleverlaan, 1989; Pickering et al., 2001), and Sorbas basin (Fortuin and Krijgsman, 2003; Martín and Braga, 1994; Riding et al., 1998). Middle Miocene sedimentary environments in the Alboran Sea are after Comas et al. (1992). **(b)** Neogene tectonic subsidence evolution for Tabernas basin and Huércal-Overa basin are from Augier (2004). The curves are obtained from backstripping techniques incorporating eustatic and paleobathymetric corrections. The question mark beneath the Sorbas basin lithofacies column indicates the potential for uncertainty and variability across the basin (see Sect. 3.2).



**Figure 7.** Distribution of (a) lower Tortonian, (b) Tortonian, (c) upper Tortonian, and (d) Messinian deposits based on geological mapping of the different basins. CF stands for Carboneras Fault, PF stands for Palomares Fault, SGF stands for South Gafarillo fault, NAF stands for North Alhambilla fault, AFZ stands for Alpujarras fault zone, BB stands for Baza basin, GB stands for Guadix basin, AB stands for Alanzora basin, HOB stands for Huércal-Óvera basin, VB stands for Vera basin, SB stands for Sorbas basin, TB stands for Tabernas basin, and AC stands for Alpujarras Corridor.

tal extension reflects a combination of pure normal faulting regime ( $\sigma_2$  horizontal and oriented NW–SE or WNW–ESE; 73 % of stress tensors) and strike-slip faulting regime ( $\sigma_2$  vertical to steeply dipping and  $\sigma_1$  horizontal and striking NNW–SSE; 27 % of stress tensors). N–S to NW–SE compression is also reported in the HOB associated with incipient syn-form and depocentre, which is dated to the lower Tortonian coeval with the prominent E–W and WSW–ENE extension (e.g. Pedrera et al., 2010).

We describe below, based on a selection of outcrops in the vicinity of the contact between Tortonian basins and major metamorphic domes, the expression of E–W and NW–SE extensional faulting in the field. We then discuss how they are linked to the regional stress regimes.

#### 4.2 E–W-trending faults: evidence for pre-Tortonian oblique extension?

In Tortonian intramontane basins, one of the main set of faults is represented by E–W-directed faults, including ENE–WSW to ESE–WNW sets. North of the Alpujarras Corridor (AC), 3 km to the NE of Canjáyar, the contact between the basal Tortonian conglomerates and the series of Alpujarride complex is exposed in the Rambla de Tices. It is shaped

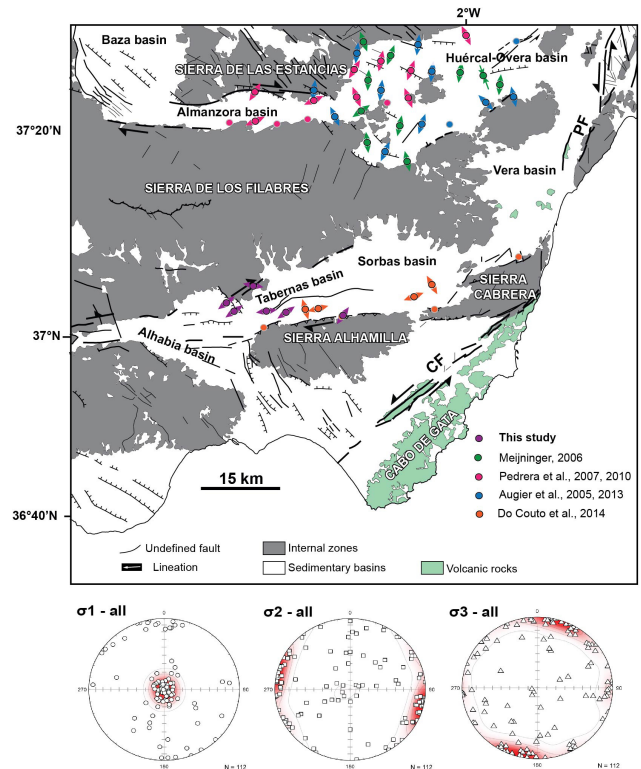


**Figure 8.** Synthesis of stress regimes resolved from fault slip data inversion in Tortonian basins. Colour-coded circles with arrows depict tectonic sites where extension (given as arrows) is horizontal (pure extensional or strike-slip stress regimes). Sites where reverse tectonic regimes prevail are shown as circles highlighted in grey. Below, stereoplots of paleostresses  $\sigma_1$ ,  $\sigma_2$ , and  $\sigma_3$  show a compilation of all brittle tectonic regimes extracted from Table S1. Collectively they define a prominent extension oriented NNE–SSW with a subordinate E–W-striking extension. CF stands for Carboneras Fault. PF stands for Palomares Fault.

by a 2 m thick fault zone (Fig. 9a, b) striking north 100° E, which has a normal sense of slip with a right-lateral strike-slip component (Fig. 9c). It consists of cataclastic breccias and sheared blocks (boudins) of the host rocks (Fig. 9d). This major fault is found along the 65 km long Alpujarras fault zone described by Martínez-Martínez (2006) as a major strike-slip dextral transfer zone south of the Sierra Nevada that accommodates both W–SW extension and dextral movement. It is mechanically consistent with NE–SW and ENE–WSW extension under a strike-slip regime as resolved nearby along the same fault system (Martínez-Martínez, 2006). Figure 9 indicates the fault is parallel to the basal Tortonian series but cuts across the Alpujarride complex. In the HOB, on the southern flank of the Sierra Limaria (Fig. 8), the unconformity between the lower Tortonian red conglomerates and the Alpujarride units (Rambla de Cordoba, 2 km NW of Arboleas, Figs. S1a, b) is found reactivated as a normal fault with a dextral shear component.

To the north of TB, a large morphological surface presents a rare exposure of the micaschist basement of the Nevado-Filábride (NF) complex allowing the study of deformation on the southern flank of the Sierra de los Filabres (Fig. 10). The deformed NF series shapes a kilometric-size antiform with an axial planar surface dipping towards the north. The steeply dipping cleavages directed NE–SW on its southern flank are deformed by numerous dextral shear zones with lengths ranging from 100 m to less than 5 m (Fig. 10b, c). In addition to isoclinal folds parallel to the main foliation that are clearly associated with an early stage of ductile E–W stretching, we recognize steeply dipping metric-size open to tight folds inclined to the NE close to the strike-slip shear zones (Fig. 10d). To the south, Tortonian conglomerates are unconformably overlying the folded NF foliation. This stratigraphic relationships and the average low dip of Tortonian strata ( $20^\circ$  to the SE) indicate that strike-slip deformation occurred before the deposition of Tortonian conglomerates and after the tilting of the NF foliation (see cross section in Fig. 10a). This argues that the transition from HP metamorphism (Burdigalian–Langhian) in the NF (Platt et al., 2006) to W-directed ductile crustal thinning and right-lateral strike-slip faulting occurred before the Tortonian, most likely around the Serravallian at 12–13 Ma. This interval is considered to mark the transition from ductile to brittle extension in the region (e.g. Augier et al., 2013). Because strike-slip faulting postdates folding of the NF foliation and is consistent with WSW–ENE oblique extension, we suggest that the Sierra de los Filabres metamorphic dome formed in a transtensional strain regime. This hypothesis conforms with prediction of transtension at the tip of the STEP fault (Le Pourhiet et al., 2012) and with model of oblique extension (see Fig. 3).

#### 4.3 NW–SE-trending normal faults

A second set is represented by NW–SE-directed normal faults (Fig. 8). They are found, for instance, bordering the NE part of Alhabia basin, where they cut across the basement and interrupt the westward continuity of the southern flank of the Sierra de los Filabres. One major fault zone of this system is well exposed in the Arroyo del Verdelecho, 7 km to the west of Tabernas, on the eastern border of the Alhabia basin (Figs. 11 and S2). From a regional point of view, this large NW–SE fault zone controls the deepening of the Tortonian basin and the position of Pliocene depocentre in its hanging wall towards the west. NW–SE normal faults also cut across the lower Tortonian conglomerates in the hanging wall, but their throw diminishes upward in the upper Tortonian margin sediments, suggesting fault activity during the late Tortonian (Fig. 11). One major fault zone is outlined by cataclastic breccias made of marbles originating from the exhumed Alpujarride complex in the Sierra de los Filabres (Fig. S2).

South of HOB (south of Arboleas), NW–SE faults are seen cutting through the late Tortonian sands and marls se-

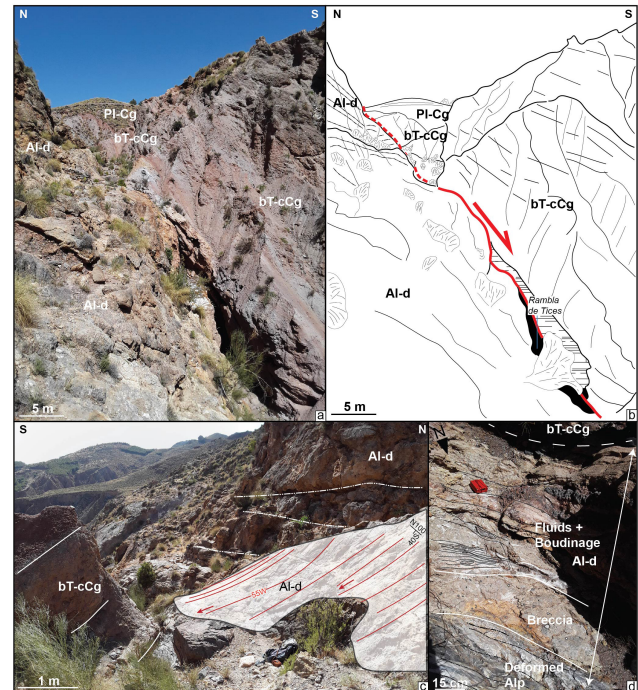


**Figure 9.** (a–b) Fault zone at the contact between the Tortonian basal conglomerates and the series of the Alpujarride complex south of AC (Rambla de Tices; see Fig. 5 for location). (c) Slickensides on the fault zone reveal a normal sense of slip with right-lateral strike-slip component found in association with (d) cataclastic breccias and sheared boudins of metamorphic and sedimentary rocks. Al-d stands for Alpujarride dolomites, bT-cCg stands for basal Tortonian continental conglomerates, and PI-Cg stands for Pliocene conglomerates. The coordinates are as follows:  $37.031944^\circ$  N,  $-2.716274^\circ$  E.

ries, indicating that NE–SW extension is at least Tortonian (Fig. S1c, d).

Both fault slip data and our own observations argue for a regional pre-Tortonian and syn-early Tortonian NNE–SSW-directed extension. This direction of extension is also found associated with less well-developed strike-slip regimes (Fig. 8). It is consistent with the D1–D2 phase of brittle deformation found in HOB (Augier et al., 2013). The fact that extension and strike-slip regimes occurred synchronously, or overlap rapidly in time, supports the view that they reflect the same large-scale tectonic setting. The reason why strike-slip faulting is less apparent in the field than expected in models in Fig. 3 is likely to reflect the fact that oblique extension is not fully partitioned between normal and strike-slip components and is actually distributed along oblique structures. Moreover, where strike-slip faults are found they are associated with narrow basins or near the contact between the cover and basement but not in the centre of HOB or TB. The NNE–SSW to NW–SE faults appear to postdate the deposition of the early Tortonian red conglomerates and are synchronous with the deposition of marine Tortonian se-

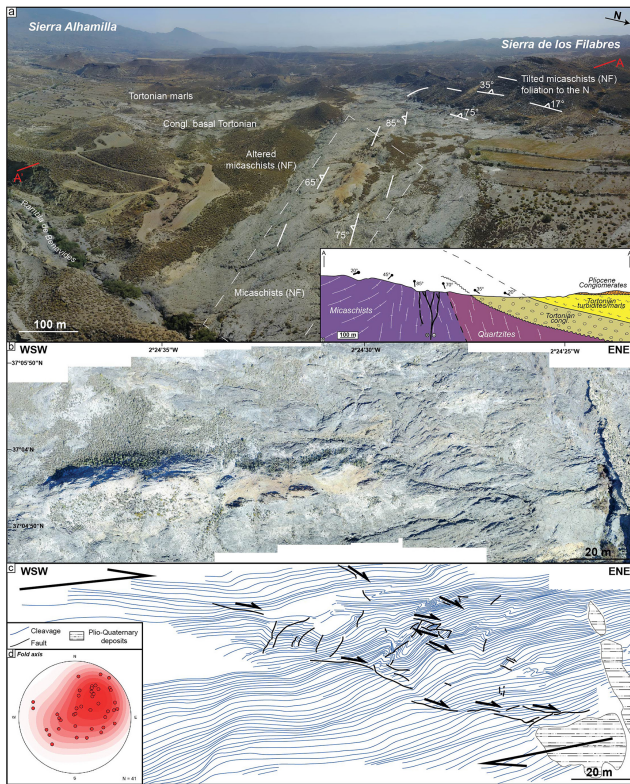


**Figure 10.** (a) Drone view taken in the SSW direction of the southern flank of the Sierra de los Filabres at the contact with the Tabernas basin (see Fig. 5 for location). Local folding of the micaschist is apparent in the right where the foliation is striking NNE–SSW and is dipping  $\sim 25^\circ$  to the E, whereas it is vertical and striking SW–NE in the centre of the studied area forming paleosurface. Local cross section highlights the unconformable contact between the Tortonian conglomerates and overlying on the basement. (b) High-resolution drone images of the paleosurface and (c) line drawing of the foliation revealing secondary folding (see (d) stereoplot of fold axes inclined to the NE) and dextral shear zones. The coordinates are as follows:  $37.082777^\circ$  N,  $-2.410544^\circ$  E.

ries (Fig. 12). These normal faults currently form half-graben filled with Plio-Quaternary deposits (Guadix, Baza, Alhabia) and are active today. However, the importance of extension-related brittle deformation over brittle compression decreases eastwards. Indeed, a late brittle compressional event oriented roughly N–S is described in the literature as a D3 brittle event (e.g. in HOB) associated with reverse and strike-slip faults (Augier et al., 2013). The post-late-Tortonian shortening is seen as responsible for fold amplification and reverse faulting on the northern limb of Sierra Alhamilla and Sierra de los Filabres and locally in the eastern part of the HOB near the termination of left-lateral strike-slip faulting evolution of the Alhama de Murcia Fault (Fig. 8).

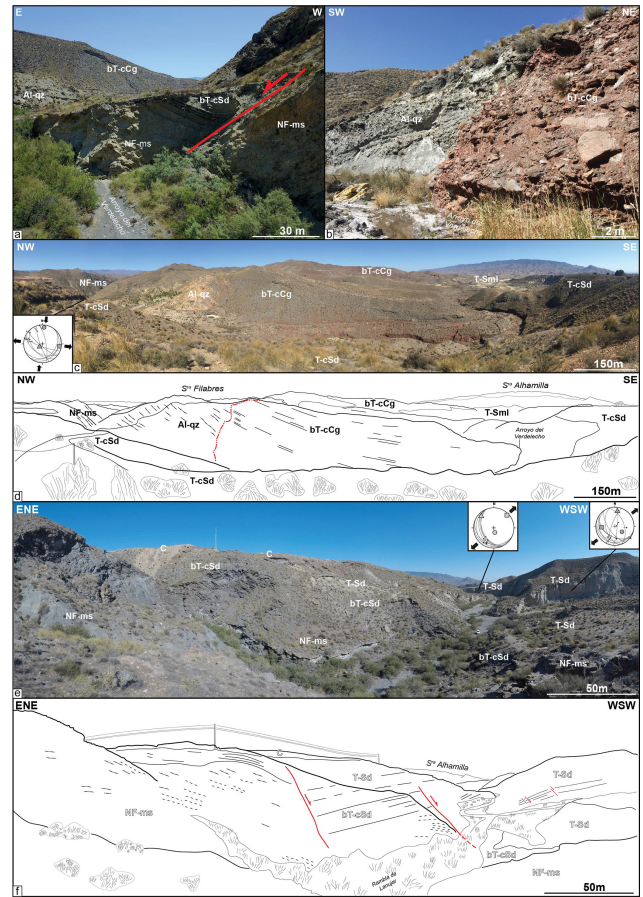


**Figure 11.** (a) Field photographs of a NW–SE normal fault at the contact between the Nevado-Filábride micaschists (footwall) and Tortonian sediments (hanging wall). (b) Stratigraphic contact between grey and red basal Tortonian continental conglomerates. These thick Tortonian series rest conformably on the Alpujarride complex (c, d). The coordinates are as follows:  $37.059507^\circ$  N,  $-2.478386^\circ$  E. (e, f) NW–SE normal faults cutting across the NF micaschists basement. These faults that also affect the early Tortonian deposits are sealed by late Tortonian deposits and are therefore syn-depositional. See Fig. 5 for location. Al-qz stands for Alpujarride quartzites, NF-ms stands for Nevado-Filábride micaschists, bT-cCg stands for basal Tortonian continental conglomerates, bT-cSd stands for basal Tortonian continental sandstones, T-cSd stands for Tortonian coarse sandstones, T-Sd stands for Tortonian sandstones, T-Sml stands for Tortonian Sandstones-marls, and C stands for calcrites. The coordinates are as follows:  $37.061279^\circ$  N,  $-2.490309^\circ$  E. Paleostress orientations are shown in Table S1.

### 5 N–S crustal-scale section across the oblique or transform margin of Alboran basin

To further examine the structural relationships between extension and strike-slip faulting across the Alboran margin, we explore 2D multichannel seismic lines acquired during the MARSIBAL 1-06 cruise (Comas and MARSIBAL1-06

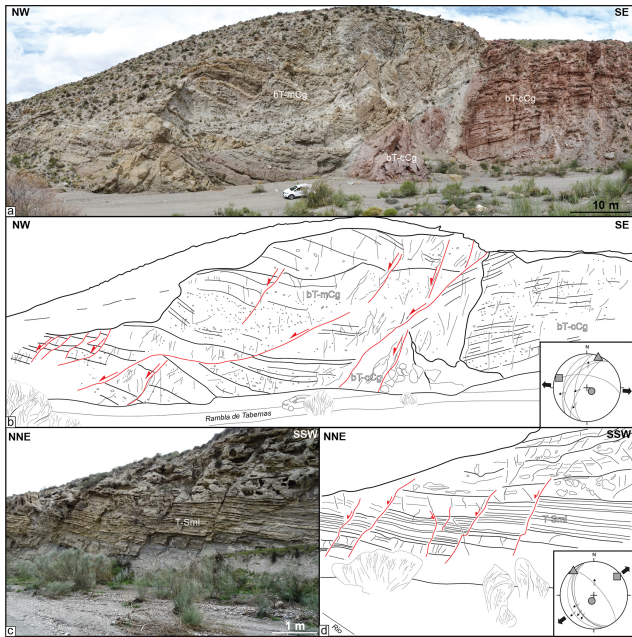


**Figure 12.** (a, b) N–S to NNE–SSW-oriented normal to dextral faults affecting the basal Tortonian continental conglomerates (bT-cCg) and marine conglomerates (bT-mCg) (Rambla de Tabernas). They form a long and tight E–W anticlinal that crosses the Tabernas basin (see Fig. 5 for location). (c, d) Several normal faults observed in Tortonian sandstones and marls (T-Sml). They are mostly oriented NNW–SSE. The coordinates are as follows: 37.041648° N, –2.399318° E. Paleostress orientations are in Table S1.

Scientific Party, 2007) and ESCI cruises (Comas et al., 1995) across the eastern Alboran basin (EAB). The studied seismic dataset consists of ~300 km worth of data from deep-penetration multichannel seismic reflection studies (12 s two-way travel time, TWTT). Here, we study two lines, namely MSB08 and MSB07 (see location in Fig. 1). For stratigraphic and structural correlations between the studied seismic lines, we used the Andalucía-A1 well (Fig. 6a) and results from Ocean Drilling Program (ODP) 977 and 978 legs (see location in Fig. 1). MSB08 is striking north 70° E, slightly oblique to the shoreline. It is close, and runs parallel, to the TM08 line of Gómez de la Peña et al. (2018). It is calibrated by the Andalucía-A1 well and ESCI-Alb1 line (Comas et al., 1995). Line MSB07 stretches in the N–S direction between the EAB in Spain and SAB to the north of Morocco parallel to line TM09 (Gómez de la Peña et al., 2018) and crosscuts line ESCI Alb2b presented in Comas et al. (1995) and Booth-Rea et al. (2007) (Fig. 1).

### 5.1 Offshore structures and stratigraphic architecture

The Carboneras Fault is well imaged north of MSB07 (Fig. 13). It forms a negative crustal-scale flower structure related to left-lateral strike-slip faulting that involves a Moho depth variation between 12 and 9–8 s TWTT after Gómez

de la Peña et al. (2018). It separates a thin continental crust to the north (25–20 km; Fig. 2) from the magmatic calc-alkaline arc crust of the EAB with a thickness of 18 km in the south (Booth-Rea et al., 2007, 2018; Gómez de la Peña et al., 2018, 2020a).

Reflection seismic data (Figs. 13, 14, 15) collectively show a stratified crust, corresponding to the sediment cover, down to 2.4–4 s TWTT, which outlines the acoustic basement with high reflectivity (B). Locally, the top basement reflector coincides with erosional palaeo-relief or high angle normal faults bounding basement highs. These faults are oriented mostly NW–SE to NE–SW and cut across the basement. We recognized on seismic images magmatic additions in the continental crust that are shaped by volcanic edifices exposed on the seafloor (e.g. Chella Bank) or slightly buried (Alboran Ridge) outlined by symmetric downlaps and onlaps of sediments. These constructions form topographic highs such as the Chella Bank on the MSB08 line (Fig. 14), the Alboran Ridge on the MSB07 line (Fig. 13), and the Maimonides Ridge on the ESCI-Alb2b line (Fig. 15). All the reflectors corresponding to layers as old as the Tortonian are onlapping against the volcanic ridges confirming that the volcanic activity occurred during middle to late Miocene times, which is shown by Duggen et al. (2008). Some reflectors up to the top Messinian (top M) onlap onto the volcanic ridges, probably as a result of Pliocene uplift.

The stratigraphy offshore, on the continental crustal domain, is defined by the recognition of five seismic stratigraphic units in the Andalucía-A1 well (Jurado and Comas, 1992) labelled I–V from top to base (Figs. 6 and 16) and separated by unconformities. The seismostratigraphic units I to V vary in thickness (Fig. 16), and their architecture is conditioned by the occurrence of basement highs and crustal-scale faults.

Below the Miocene sedimentary filling, the Andalucía-A1 well reveals ~190 m of phyllitic and quartzitic meta-sediments (2.4 to 4 s TWTT below the Alboran basin, Figs. 13 and 14) topped by Langhian to Tortonian marls (top at ~1.6 to 3.4 s TWTT below the Alboran basin) interbedded with Tortonian–Messinian tuffs and basaltic lavas. These units have been correlated in the magmatic arc crust of EAB after Gómez de la Peña et al. (2020b). The older deposits (Unit V) are Langhian–Serravallian in age and consist of clays and marls with intercalated sands and volcanoclastic deposits. The seismic facies of this Unit V are made of moderate-amplitude and low-frequency discontinuous reflections packages (Fig. 16) and are only present in the northern Alboran basin. They are correlated with volcanic series in the EAB (vY3) (Gómez de la Peña et al., 2020b). They pass upward into Serravallian sand–silty clay turbidite (Unit IV) possibly correlated with volcanic series in EAB (vY2 after Gómez de la Peña et al., 2020b). This unit exhibiting low-to moderate-amplitude, moderate-frequency drawing continuous sheeted to disrupted reflectors is unconformably overlying Unit V and locally onlaps onto the basement. The

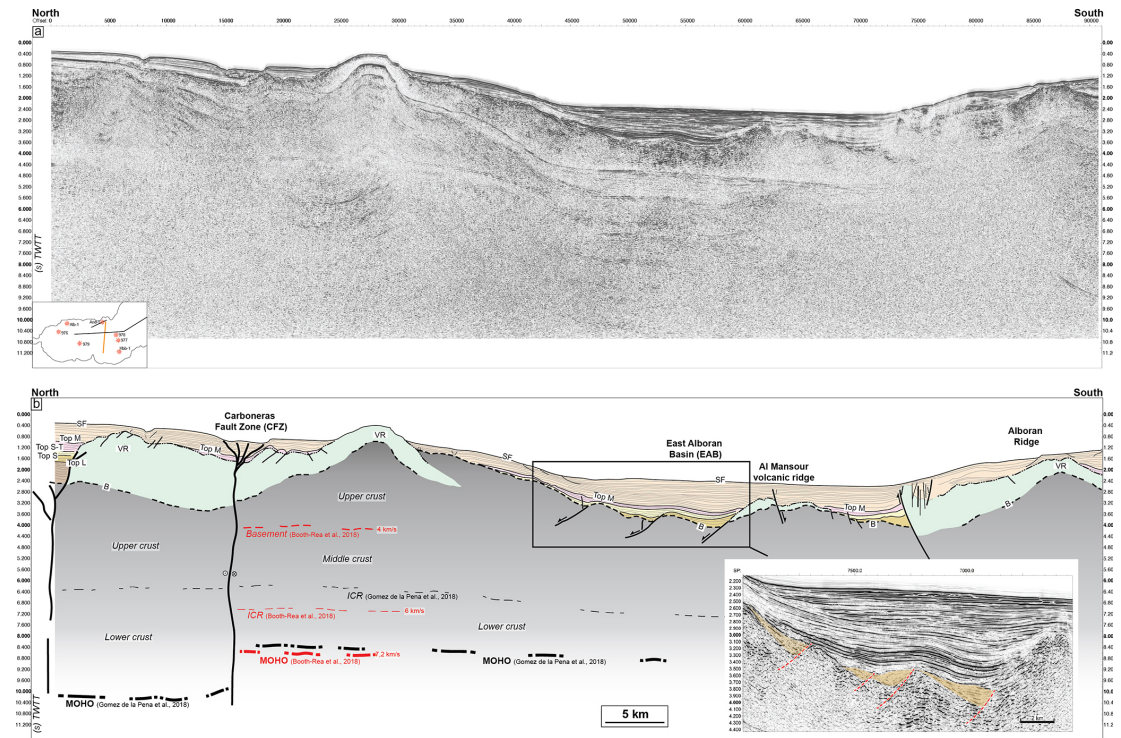


**Figure 13.** Seismic reflection line MSB07 (location in Fig. 1). Discontinuous intracrustal reflectors (ICRs) imaged between 3 and 6.5 s TWTT have been interpreted as mylonitic zones within the metamorphic basement (Carbonell et al., 1998; García-Dueñas et al., 1994; Gómez de la Peña et al., 2018). VR stands for volcanic ridge, B is the acoustic basement, Top L is the top Langian, Top S is the top Serravallian, Top S-T is the top Serravallian–Tortonian, Top M is the top Messinian, SF stands for seafloor.

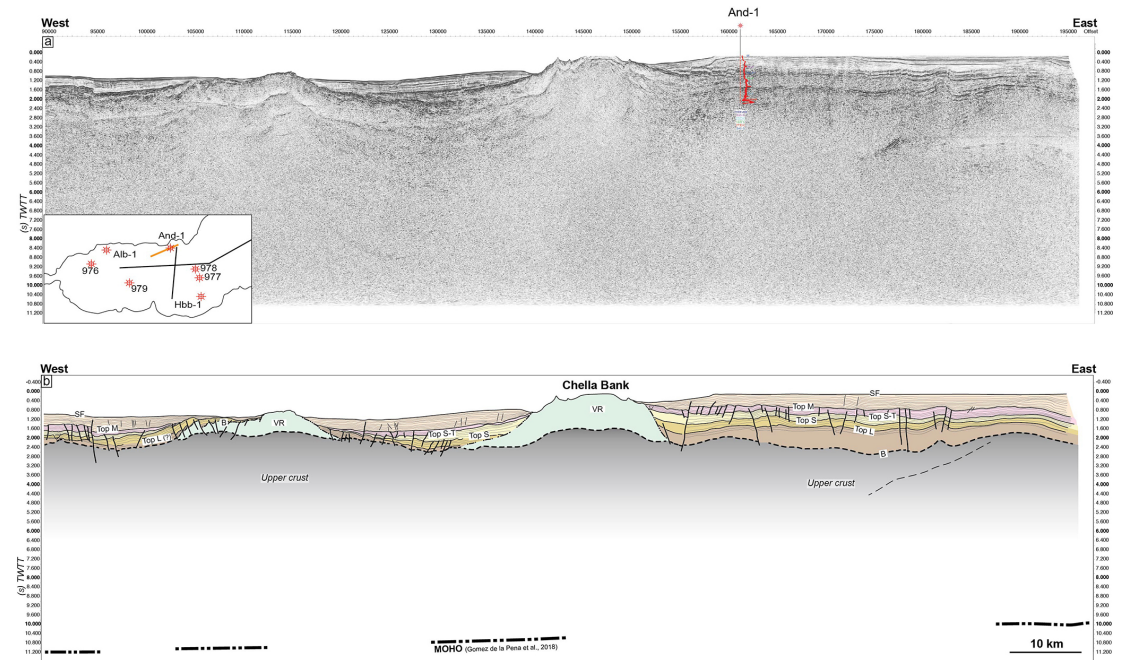


**Figure 14.** Seismic reflection line MSB08 (see location in Fig. 1). See Fig. 13 for abbreviations and Fig. S3 for a zoom on the main seismic facies recognized in the Andalucía-A1 well.

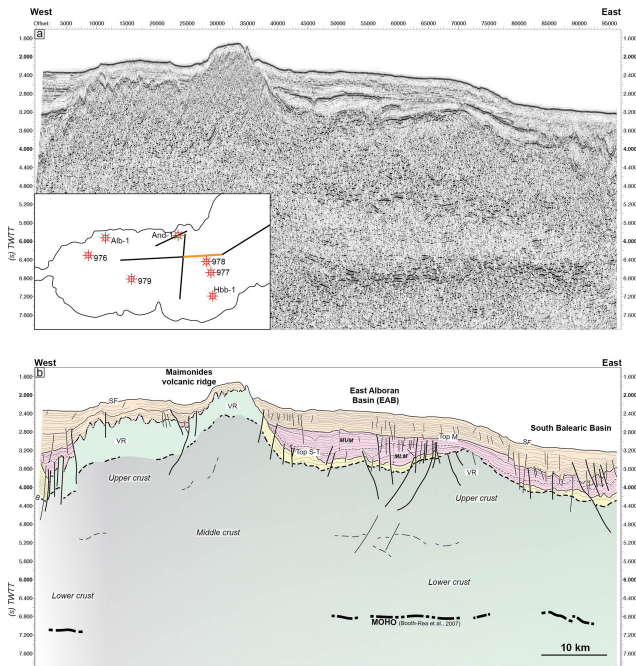


**Figure 15.** (a, b) Seismic reflection line ESCI-Alb2b and interpretation (see Fig. 1 for location). Seismic units are correlated with those defined by Booth-Rea et al. (2007). See Fig. 13 for abbreviations.

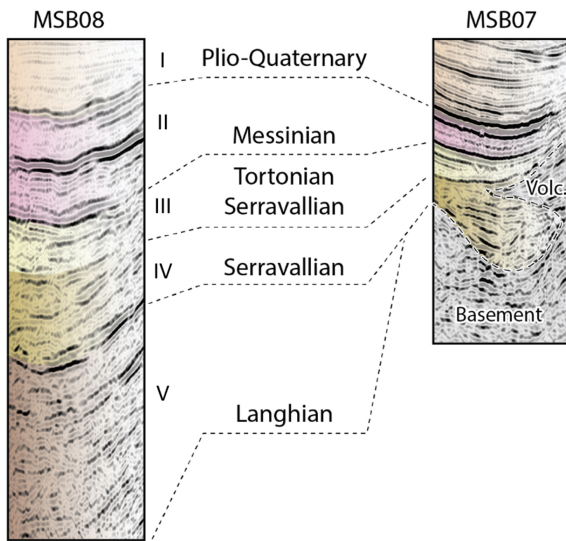


**Figure 16.** Seismic facies of units I to V seen through seismic lines MSB08 close to the shoreline and the line MSB07, located deeper in the eastern Alboran basin.

thickness of Unit IV remains rather thin in the northern and eastern Alboran basin. It cannot be properly identified in the southern Balearic basin, east of the Maimonides volcanic ridge (Fig. 15). Unit III, dated from late Serravallian to late Tortonian, is represented by sandstones interbedded with volcano-clastic levels that correlate in EAB with the vol-

canic vY1 unit. Unit III contains internal reflections characterized by low- to moderate-amplitude, moderate-frequency continuous sheeted reflectors. Its thickness remains relatively constant from the NAB to the EAB and is identified beneath the Messinian Unit II in the southern Balearic basin. Unit II corresponds to the Messinian evaporite, carbonate, volcanic, and volcanoclastic deposits interbedded with fine-grained sediments and is equivalent to unit III of Gómez de la Peña et al. (2020b) in EAB. Seismic facies of Unit II are marked in the Alboran domain by lower amplitudes and lower-frequency reflectors. In ESCI-Alb2b line, Unit II increases drastically east of the Maimonides Ridge, which delimits the western boundary of the salt deposits in the western Mediterranean basin during the Messinian Salinity Crisis (Haq et al., 2020). Unit II is topped by Unit I, which is made of Pliocene to Quaternary clays and sandstones and is correlated with units II and I in EAB (Gómez de la Peña et al., 2020b). Unit I is marked by thinly bedded, mostly parallel, high-frequency and low-amplitude reflectors (Fig. 15). Its thickness fluctuates in response to sedimentary processes (Juan et al., 2016).

Along line MSB08 (Fig. 14) the Langhian–Serravallian (Unit V) is a maximum of 1600 m thick (using a P-wave velocity of  $3.2 \text{ km s}^{-1}$  calculated within the Andalucía-A1 well). In EAB, south of the Carboneras fault zone, the total thickness of Unit V is only  $\sim 300 \text{ m}$  on MSB07 (Fig. 13) and is absent in ESCI-Alb2b (Fig. 15). The Serravallian–Tortonian (units IV–III) interval shows only very limited sediment accumulation ( $\sim 300 \text{ m}$ ) except near the NW–SE-oriented normal faults where growth geometries are visible. These normal faults are sealed by the Tortonian–Messinian deposits, indicating a syn-sedimentary faulting during the middle Miocene (Fig. 13). With respect to onshore observations, this sedimentary infill is more continuous and is also much thinner compared to TB and HOB, where they are represented by thick conglomerates and marls or turbidites ( $> 1 \text{ km}$ ) (Fig. 7) and are eroded or not deposited along the axes of the metamorphic domes. The Messinian deposits (Unit II) are  $\sim 150\text{--}350 \text{ m}$  thick north of CF (MSB07-08; Figs. 13, 14) and increase to about 1200 m eastward in the eastern EAB (ESCI-Alb2b; Fig. 15) and in the Algero-Balearic basin (Gómez de la Peña et al., 2020b). The top Messinian reflector is topped by thick horizontal sedimentary strata, with a maximum thickness of 1.2 s TWTT ( $\sim 2.4 \text{ km}$  assuming a velocity of  $2 \text{ km s}^{-1}$ ) on line MSB07, suggesting an important channel system during the Pliocene.

The Pliocene to Quaternary series are poorly deformed except in the vicinity of CF and near the Alboran Ridge where this is associated with an S-dipping reverse fault (Fig. 13). This late and still-active compressional tectonic activity is revealed by the overthrusting of the SAB over the south margin of the EAB (e.g. Martínez-García et al., 2011).

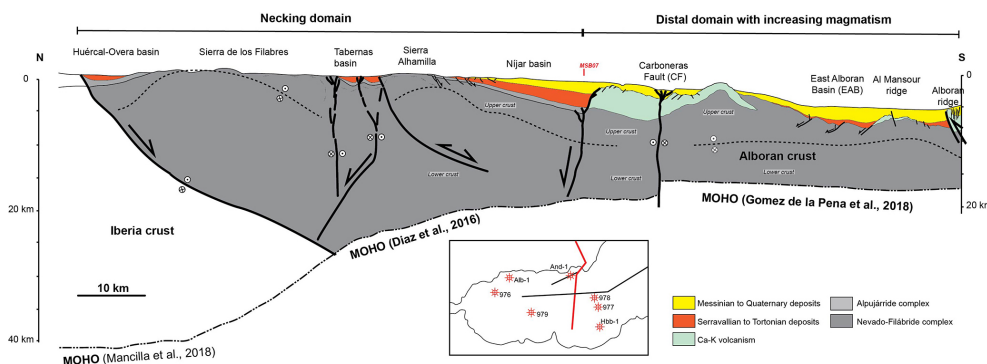


**Figure 17.** Crustal-scale cross section of the Alboran margin in the eastern Betics interpreted based on onshore and offshore constraints presented in the text. Note that in the necking domain the extension of faults downwards to Moho depths is not imaged on the seismic data and therefore is largely inspired by inferences from 3D numerical models (see Fig. 3).

## 5.2 N–S crustal cross section of the Alboran margin accounting for strike-slip faulting

Based on subsurface constraints and field data, in Fig. 17 we present a crustal-scale section across the rifted margin, from the Sierra de las Estancias and Huércal-Overa basin (HOB) to the Alboran ridge, that represents the inverted southern margin of the EAB. The proximal margin, where the crust is 30–35 km thick, is defined to the north by the transition between the southern Iberia margin and the metamorphic domain of the Alboran basement exposed in the Sierra de las Estancias. This continental domain preserves part of the crustal thickness acquired during former Betic orogenic phase that has been little involved in crustal thinning. The onset of crustal thinning to the south coincides with the position of the lithospheric tear fault documented by seismology (Fig. 4; Mancilla et al., 2015a) and is recorded by the formation of asymmetric basins of the HOB and TB, shaping the upper neck domain. Orthogonal and oblique extension in this domain is accommodated by normal and strike-slip faulting during the Tortonian. From the Sierra de los Filabres to the south, the thickness of the continental crust reduces to 25 km in the Tabernas basin along the Alpujarras strike-slip fault zone and below the Sierra Alhamilla (Fig. 17). The Nijar basin depicts the transition towards offshore distal domains where the continental crust reaches a thickness of 20 km. The Tortonian and Messinian marine sediments are also thicker. It is worth noting that a number of volcanic bodies offshore (e.g. Chella Bank on MSB08) accompany crustal thinning of the continental crust. The Carboneras Fault (CF) brings crusts with different thicknesses and compositions into contact. South of the CF, the crustal thickness of the EAB is 18 km, and seismic velocities, especially the occurrence of a high- $V_p$  lower crust, have been considered to indicate that the EAB is floored by a magmatic arc crust (Gómez de la Peña et al., 2018, 2020) formed in a supra-subduction context above the subducting Alboran slab (Booth-Rea et al., 2018). The crustal thickness of the EAB

is compatible with crustal thinning of the continental margin, and the occurrence of NW–SE-trending faults also recognized onshore despite being slightly older (Serravallian–Tortonian) suggests that the EAB formed under the same back-arc extension setting relative to westward slab retreat (as did the whole Alboran margin). Thus, the magmatic arc crust of the EAB could represent voluminous magmatic intrusions (e.g. Al Mansour dacite or Alboran Ridge rhyolite dated to ca. 9 Ma; Duggen et al., 2004; Tenderso-Salmerón et al., 2022; Fig. 17) formed on the distal rifted margin of the Alboran Ridge. The investigation of the causes of calc-alkaline magmatism is beyond the scope of this study, but we suspect it reflects post-subduction arc magmatism induced by remelting during extension and delamination of a metasomatized wedge of mantle lithosphere formed during a previous subduction event (e.g. Richards, 2009). The fact that calc-alkaline magmatism around 10 Ma that is 10 to 5 Myr after the onset of upper plate extension in the Betic–Alboran region supports this view. Note that in contrast to Gómez de la Peña et al. (2020) and Booth-Rea et al. (2018), we implicitly assume the magmatic arc crust of EAB is not a newly formed crust but rather represents a thinned continental crust later intruded by calc-alkaline magmas. Different crustal domains are expected across a rifted margin that has involved a variable amount and different types of mantle-derived magmatism, especially if delamination or subduction occurred during extension. The observation of contrasting types of crustal domains now juxtaposed in the N–S direction is also related to the fact that extension is oriented perpendicular to the section.

Crustal shortening in Fig. 17 is distributed across the north-vergent reverse faults below the Alboran Ridge on the northern limb of Sierra de Alhamilla and the CF strike-slip fault zone.



## 6 Implications

The question of whether the Miocene tectonic evolution of the Betics reflects crustal thinning associated with oblique back-arc rifting as suggested from present-day strain patterns is unclear in the literature. We found based on a comparison between numerical models and basin analyses, fault kinematics, and the structure of the margin in the eastern Betics that there is compelling evidence that crustal thinning was controlled by oblique extension. Oblique rifting operated since at least the middle Miocene in relation to Alboran slab retreat below the Alboran basin and is kinematically associated with slab tearing and delamination below the central and eastern Betics.

One of the most striking tectonic features of the Alboran margin (Fig. 17) is the abrupt N–S crustal thinning oblique to the direction of slab rollback. The history of sediment infill and rates of subsidence in intramontane basins (Figs. 6 and 7), combined with the analyses of fault slip data (Fig. 8) and structural data offshore (Fig. 13), confirm that brittle extension oriented from north 20° E to E–W occurred during an interval spanning from the Serravallian–early Tortonian to the late Tortonian (14–8 Ma) (Fig. 18). This extension is found to be associated with both normal and strike-slip regimes. Field tectonic data reveal that north 20° E extension is more represented in HOB while the ENE–WSW to E–W extension is found to be related to the evolution of the Almanzora fault zone, Alpujarras fault zone, and Tabernas basin flanking the metamorphic domes (Table S1). There is additional evidence that E–W-directed dextral strike-slip faulting occurred during the Tortonian to the south and west of the HOB. These large-scale transfer fault zones positioned on the slab edge accommodate the differential westward extension that are later cut by Tortonian NW–SE faults. This second set of faults is also observed in the magmatic crust of the EAB offshore, but seismic data indicate they are Serravallian–Tortonian in age and therefore older than those identified onshore. We suggest that NW–SE normal faulting could have initiated in the EAB and then migrated towards the necking domain as slab retreat progressed and the width of the region affected by crustal thinning widened (Fig. 18). Subsidence during the Serravallian–Tortonian appears to have been lower in the EAB compared to intramontane basins onshore. This suggests that the isostatic effect of crustal thinning was compensated by a thermal anomaly in the mantle, heralding the Ca–K magmatism at 11–7 Ma (Duggen et al., 2004, 2008).

Several key tectonic features found in the eastern Betics are predicted by 3D models of oblique extension (Fig. 3). They include E–W-trending normal faults that are prevalent on the upper neck domain (i.e. Sierra de las Estancias and HOB) and E–W strike-slip faults (Almanzora and Alpujarras fault zones). NW–SE normal faults are associated with more distal domains on the continental margin where crustal thinning is the highest offshore, south of Nijar basin, and in the EAB.

Tectonic inversion seems, in contrast, to have been increasingly more important when approaching the Carboneras and Palomares strike-slip faults in the east since the late Tortonian.

Ductile thinning associated with the formation of metamorphic domes and exhumation of HP rocks is dated to 23 to 16 Ma (Platt et al., 2003; Booth-Rea et al., 2015). This provides a time constraint for the beginning of oblique extension and westward slab rollback. Deformation at the future location of the tear fault was probably initially diffuse and resulted in an immature oblique rift system in the south combined with thrusting in the external zones to the north (Fig. 18). In the Serravallian (14–13 Ma), accompanying slab steepening, localization of slab tearing, and propagation of thrusting in external zones led to oblique extension spread over the whole central Betics. At this time, metamorphic domes exhumed to upper crustal levels (e.g. Vázquez et al., 2011) and recorded the transition from ductile shearing to brittle faulting (Fig. 18). Brittle E–W-directed stretching and dextral transcurrent deformation formed at this time. The late- and post-Tortonian times (from 10–8 Ma) mark a change in the tectonic evolution of the Betics and Alboran domain possibly related to the onset of slab detachment in the eastern Betics (van Hinsbergen et al., 2014; Do Couto et al., 2014; Mancilla et al., 2015a; Martínez-García et al., 2017; d’Acremont et al., 2020; García-Castellanos and Villaseñor, 2012; Spakman et al., 2018). This event is synchronous with the indentation by the magmatic arc crust of the EAB in the Águilas Arc (Ercilla et al., 2022), amplification of the metamorphic domes in the vicinity of the EBSZ (e.g. Alhamilla), transition from Ca–K in EAB to more alkaline magmatism in eastern Betics and at a regional scale with exhumation in northern Iberia (Rat et al., 2022), and N–S shortening in northern Africa (Jolivet et al., 2021a) (Fig. 18).

In this model, ductile stretching and ductile detachment associated with the development of the domes are the expression of oblique E–W extension. It provides a coherent scheme linking the formation of E–W-directed basins in the brittle field associated with strike-slip faulting and NW–SE and NNW–SSE sedimentary basins (Guadix, Baza, Alhabia) formed in transtension during the Tortonian. As such, the oblique extension is closely associated with STEP faulting required by westward slab rollback. The oblique rifting model we propose explains the formation of the metamorphic domes and intermontane basins and provides insight into crustal deformation, which is broadly consistent with the geodynamic models of slab rollback and tearing since 20 Ma that have been previously proposed for the Alboran basin (Chertova et al., 2014; Spakman et al., 2018). In the latter models, however, the ENE–WSW extension in the central and eastern Betics is related to differential absolute motions between Iberia and the slab decoupled from Iberia by slab tearing. In our scenario, oblique extension is entirely related to westward lateral rollback. It can not be excluded, however, that the effect of mantle-derived slab dragging increased dur-

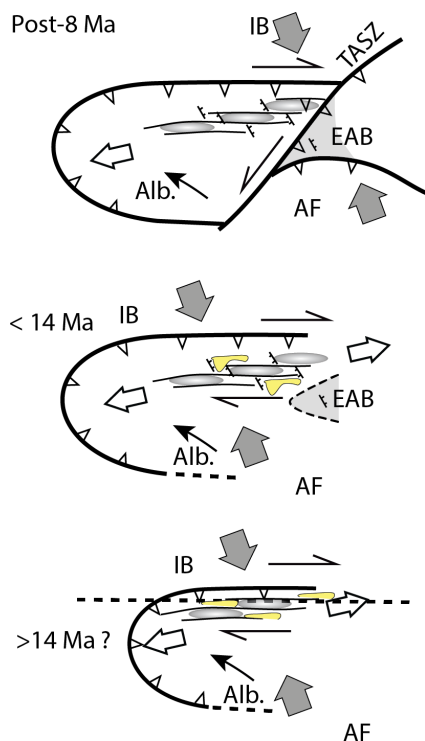


**Figure 18.** Tectonic model of the evolution of the northern margin of the Alboran Rift. Large grey and white arrows depict shortening parallel to the Africa–Iberia (AF–IB) convergence and the highly oblique extension, respectively. The thin black arrows show the motion of the Alboran basin relative to IB taken from Fig. 4. Half arrows depict distributed strike-slip faulting in the Betics. NW–SE-directed normal fault and strike-slip basins (yellow) are consistent with the oblique extension. Grey-shaded ellipses represent the metamorphic domes. TASZ represents a simplified representation of the Trans-Alboran Shear Zone. We also indicated the EAB, which mostly formed ca. 9 Ma (Duggen et al., 2004; Booth-Rea et al., 2018).

ing the late extensional stage, from 14 to 13 Ma, when slab tearing localized.

Mid-Miocene high-pressure metamorphism documented in the central Betics (e.g. Platt et al., 2013) was synchronous with slab steepening and subduction that was underway during oblique back-arc extension (Fig. 18). The case of exhumation of high-pressure rocks in the oblique convergence setting associated with near-parallel orogen extension is also documented in other active orogens like Taiwan (Conand et al., 2020).

This highly oblique northern Alboran margin differs from typical transform fault margins such as those associated with the Atlantic Ocean because it accommodates variations in intra-plate extensional movements triggered by slab rollback and not variations in spreading rates. Strike-slip faults may have originated as low-angle normal faults that were later reactivated as thrusts during margin inversion. Similar observations, including metamorphism, strike-slip faulting,

high geothermal gradients, and volcanism have been made in Seram, north of the Banda Arc, which represents another example of extremely thinned crust formed perpendicular to the direction of the slab rollback (Pownall et al., 2013). Such a narrow rifted margin associated with a lithospheric STEP fault defines a class of oblique margin that is expected to be barely preserved in the geological record due to the transient nature of retreating subduction systems.

*Data availability.* All data are presented in the Supplement.

*Supplement.* The supplement related to this article is available online at: <https://doi.org/10.5194/se-14-1221-2023-supplement>.

*Author contributions.* ML and FM conceptualized the study, prepared figures and tables, compiled and interpreted field structural data, and wrote the paper. DC provided and interpreted the seismic lines, reviewed the text, and contributed to the writing. AJ carefully examined the implementation of the numerical results and reviewed the text. EM, SC, and VM supervised and coordinate the different project tasks and reviewed the text.

*Competing interests.* The contact author has declared that none of the authors has any competing interests.

*Disclaimer.* Publisher’s note: Copernicus Publications remains neutral with regard to jurisdictional claims made in the text, published maps, institutional affiliations, or any other geographical representation in this paper. While Copernicus Publications makes every effort to include appropriate place names, the final responsibility lies with the authors.

*Special issue statement.* This article is part of the special issue “(D)rifting into the future: the relevance of rifts and divergent margins in the 21st century”. It is not associated with a conference.

*Acknowledgements.* Víctor Tintero Salmerón, Guillermo Booth-Rea, Jordan Phethean, and an anonymous reviewer are warmly thanked for their comments that greatly improved the manuscript. Susanne Buitter is thanked for handling the manuscript. The stereogram results were obtained using Win-Tensor, a software developed by Damien Delvaux, Royal Museum for Central Africa, Tervuren, Belgium (Delvaux and Sperner, 2003). The processed seismic data were interpreted using Kingdom IHS Suite© software. This research benefited from discussions and support of OROGEN project, an academic–industry research consortium between TO-TAL, CNRS, and BRGM.

*Financial support.* This research has been supported by TOTAL, CNRS, and BRGM (OROGEN project grant).

*Review statement.* This paper was edited by Susanne Buitter and reviewed by Víctor Tintero Salmerón, Guillermo Booth-Rea, and one anonymous referee.

## References

- Angrand, P. and Mouthereau, F.: Evolution of the Alpine orogenic belts in the Western Mediterranean region as resolved by the kinematics of the Europe-Africa diffuse plate boundary, *Bsgf – Earth Sci. Bull.*, 192, 42, <https://doi.org/10.1051/bsgf/2021031>, 2021.
- Argus, D. F., Gordon, R. G., and DeMets, C.: Geologically current motion of 56 plates relative to the no-net-rotation reference frame. *Geochemistry, Geophysics, Geosystems*, 12, <https://doi.org/10.1029/2011gc003751>, 2011.
- Augier, R.: Evolution tardi-orogénique des Cordillères Bétiques (Espagne): apports d'une étude intégrée 1 Vol., 400 p., tel-00008744, 2004.
- Augier, R., Agard, P., Monié, P., Jolivet, L., Robin, C., and Booth-Rea, G.: Exhumation, doming and slab retreat in the Betic Cordillera (SE Spain): in situ  $^{40}\text{Ar}/^{39}\text{Ar}$  ages and P–T–d–t paths for the Nevado-Filabride complex, *J. Metamorph. Geol.*, 23, 357–381, <https://doi.org/10.1111/j.1525-1314.2005.00581.x>, 2005.
- Augier, R., Booth-Rea, G., Agard, P., Martínez-Martínez, J. M., Jolivet, L., and Azañón, J. M.: Exhumation constraints for the lower Nevado-Filabride Complex (Betic Cordillera, SE Spain): a Raman thermometry and Tweek multiequilibrium thermobarometry approach, *Bsgf – Earth Sci. Bulletin*, 176, 403–416, <https://doi.org/10.2113/176.5.403>, 2005a.
- Augier, R., Jolivet, L., Do Couto, D., and Negro, F.: From ductile to brittle, late- to post-orogenic evolution of the Betic Cordillera: Structural insights from the northeastern Internal zones, *Bsgf – Earth Sci. Bulletin*, 184, 405–425, <https://doi.org/10.2113/gssgfbull.184.4-5.405>, 2013.
- Augier, R., Jolivet, L., and Robin, C.: Late Orogenic doming in the eastern Betic Cordilleras: Final exhumation of the Nevado-Filabride complex and its relation to basin genesis, *Tectonics*, 24, TC4003, <https://doi.org/10.1029/2004tc001687>, 2005b.
- Badji, R., Charvis, P., Bracene, R., Galve, A., Badsji, M., Ribodetti, A., Benaissa, Z., Klingelhoefer, F., Medaouri, M., and Beslier, M.-O.: Geophysical evidence for a transform margin offshore Western Algeria: a witness of a subduction-transform edge propagator?, *Geophys. J. Int.*, 200, 1029–1045, <https://doi.org/10.1093/gji/ggu454>, 2014.
- Barcos, L., Balanyá, J. C., Díaz-Azpiroz, M., Expósito, I., and Jiménez-Bonilla, A.: Kinematics of the Torcal Shear Zone: Transpressional tectonics in a salient-recess transition at the northern Gibraltar Arc, *Tectonophysics*, 663, 62–77, <https://doi.org/10.1016/j.tecto.2015.05.002>, 2015.
- Baudouy, L., Haughton, P. D. W., and Walsh, J. J.: Evolution of a Fault-Controlled, Deep-Water Sub-Basin, Tabernas, SE Spain, *Front. Earth Sci.*, 9, 767286, <https://doi.org/10.3389/feart.2021.767286>, 2021.
- Bessière, E., Jolivet, L., Augier, R., Scaillet, S., Précigout, J., Azañón, J.-M., Crespo-Blanc, A., Masini, E., and Do Couto, D.: Lateral variations of pressure-temperature evolution in non-cylindrical orogens and 3-D subduction dynamics: the Betic-Rif Cordillera example, *Bsgf – Earth Sci. Bull.*, 192, 8, <https://doi.org/10.1051/bsgf/2021007>, 2021.
- Bezada, M. J., Humphreys, E. D., Toomey, D. R., Harnafi, M., Dávila, J. M., and Gallart, J.: Evidence for slab rollback in westernmost Mediterranean from improved upper mantle imaging, *Earth Planet. Sci. Lett.*, 368, 51–60, <https://doi.org/10.1016/j.epsl.2013.02.024>, 2013.
- Booth-Rea, G., Martínez-Martínez, J. M., and Giaconia, F.: Continental subduction, intracrustal shortening, and coeval upper-crustal extension: P-T evolution of subducted south Iberian paleomargin metapelites (Betics, SE Spain), *Tectonophysics*, 663, 122–139, <https://doi.org/10.1016/j.tecto.2015.08.036>, 2015.
- Booth-Rea, G., Ranero, C. R., and Grevemeyer, I.: The Alboran volcanic-arc modulated the Messinian faunal exchange and salinity crisis, *Sci. Rep.*, 8, 13015, <https://doi.org/10.1038/s41598-018-31307-7>, 2018.
- Booth-Rea, G., Ranero, C. R., Martínez-Martínez, J. M., and Grevemeyer, I.: Crustal types and Tertiary tectonic evolution of the Alborán sea, western Mediterranean, *Geochem. Geophys. Geosyst.*, 8, Q10005, <https://doi.org/10.1029/2007gc001639>, 2007.
- Booth-Rea, G., Azañón, J.-M., Azor, A., and García-Dueñas, V.: Influence of strike-slip fault segmentation on drainage evolution and topography. A case study: the Palomares Fault Zone (southeastern Betics, Spain), *J. Struct. Geol.*, 26, 1615–1632, <https://doi.org/10.1016/j.jsg.2004.01.007>, 2004a.
- Booth-Rea, G., Azañón, J. M., and García-Dueñas, V.: Extensional tectonics in the northeastern Betics (SE Spain): case study of extension in a multilayered upper crust with contrasting rheologies, *J. Struct. Geol.*, 26, 2039–2058, <https://doi.org/10.1016/j.jsg.2004.04.005>, 2004b.
- Borque, M. J., Alzola, A. S., Martín-Rojas, I., Alfaro, P., Molina, S., Cintas, S. R., Caderot, G. R., Lacy, C., Avilés, M., Olmo, A. H., Tortosa, F. J. G., Estévez, A., and Gil, A. J.: How Much Nubia-Eurasia Convergence Is Accommodated by the NE End of the Eastern Betic Shear Zone (SE Spain)? Constraints From GPS Velocities, *Tectonics*, 38, 271–1839, <https://doi.org/10.1029/2018tc004970>, 2019.
- Braga, J. C., Martín, J. M., and Quesada, C.: Patterns and average rates of late Neogene–Recent uplift of the Betic Cordillera, SE Spain, *Geomorphology*, 50, 3–26, [https://doi.org/10.1016/s0169-555x\(02\)00205-2](https://doi.org/10.1016/s0169-555x(02)00205-2), 2003.
- Carbonell, R., Sallares, V., Pous, J., Dañobeitia, J. J., Queralt, P., Ledo, J. J., and Dueñas, V. G.: A multidisciplinary geophysical study in the Betic chain (southern Iberia Peninsula), *Tectonophysics*, 288, 137–152, [https://doi.org/10.1016/s0040-1951\(97\)00289-8](https://doi.org/10.1016/s0040-1951(97)00289-8), 1998.
- Chertova, M. V., Spakman, W., Geenen, T., Berg, A. P., and Hinsbergen, D. J. J.: Underpinning tectonic reconstructions of the western Mediterranean region with dynamic slab evolution from 3-D numerical modeling, *J. Geophys. Res.-Solid Earth*, 119, 5876–5902, <https://doi.org/10.1002/2014jb011150>, 2014.
- Clark, S. J. P. and Dempster, T. J.: The record of tectonic denudation and erosion in an emerging orogen: an apatite fission-track study of the Sierra Nevada, southern Spain, *J. Geol. Soc.*, 166, 87–100, <https://doi.org/10.1144/0016-76492008-041>, 2009.

- Comas, M. C., Dañobeitia, J. J., Alvarez-Maron, J., and Soto, J. I.: Crustal reflections and structure in the Alboran Basin. Preliminary results of the ESCI-Alboran survey, *Rev. Soc. Geol. Esp.*, 8, 529–542, 1995.
- Comas, M. C., García-Dueñas, V., and Jurado, M. J.: Neogene tectonic evolution of the Alboran Sea from MCS data, *Geo.-Mar. Lett.*, 12, 157–164, <https://doi.org/10.1007/bf02084927>, 1992.
- Comas, M. and MARSIBAL 1-06 Scientific Party: Preliminary results of Marsibal 1-06 cruise in the Alboran and western Algero-Balearic basins, *Geophys. Res. Abstr.*, 9, 10871, SRef-ID 1607-7962/gra/EGU2007-A-10871, 2007.
- Conand, C., Mouthereau, F., Ganne, J., Lin, A. T., Lahfid, A., Daudet, M., Mesalles, L., Giletycz, S., and Bonzani, M.: Strain Partitioning and Exhumation in Oblique Taiwan Collision: Role of Rift Architecture and Plate Kinematics, *Tectonics*, 39, e2019TC005798, <https://doi.org/10.1029/2019tc005798>, 2020.
- Crespo-Blanc, A., Comas, M., and Balanyá, J. C.: Clues for a Tortonian reconstruction of the Gibraltar Arc: Structural pattern, deformation diachronism and block rotations, *Tectonophysics*, 683, 308–324, <https://doi.org/10.1016/j.tecto.2016.05.045>, 2016.
- d’Acremont, E., Lafosse, M., Rabaute, A., Teurquety, G., Couto, D. D., Ercilla, G., Juan, C., Lépinay, B. M., Lafuerza, S., Galindo-Zaldivar, J., Estrada, F., Vazquez, J. T., Leroy, S., Poort, J., Ammar, A., and Gorini, C.: Polyphase Tectonic Evolution of Fore-Arc Basin Related to STEP Fault as Revealed by Seismic Reflection Data From the Alboran Sea (W-Mediterranean), *Tectonics*, 39, e2019TC005888, <https://doi.org/10.1029/2019tc005888>, 2020.
- Dalziel, I. W. D., Lawver, L. A., Norton, I. O., and Gahagan, L. M.: The Scotia Arc: Genesis, Evolution, Global Significance, *Annu. Rev. Earth Pl. Sc.*, 41, 767–793, <https://doi.org/10.1146/annurev-earth-050212-124155>, 2013.
- Daudet, M., Mouthereau, F., Bricchau, S., Crespo-Blanc, A., Gautheron, C., and Angrand, P.: Tectono-Stratigraphic and Thermal Evolution of the Western Betic Flysch: Implications for the Geodynamics of South Iberian Margin and Alboran Domain, *Tectonics*, 39, e2020TC006093, <https://doi.org/10.1029/2020tc006093>, 2020.
- Delvaux, D. and Sperner, B.: New aspects of tectonic stress inversion with reference to the TENSOR program, *Geol. Soc., Lond., Spéc. Publ.*, 212, 75–100, <https://doi.org/10.1144/gsl.sp.2003.212.01.06>, 2003.
- Dewey, J. F.: Extensional collapse of orogens, *Tectonics*, 7, 1123–1139, <https://doi.org/10.1029/tc007i006p01123>, 1988.
- Dewey, J.F., Helman, M.L., Knott, S.D., Turco, E., Hutton, D.H.W.: Kinematics of the western Mediterranean, *Geol. Soc. London Spec. Pub.*, 45, 265–283, <https://doi.org/10.1144/gsl.sp.1989.045.01.15>, 1989.
- Diaz, J., Gallart, J., and Carbonell, R.: Moho topography beneath the Iberian-Western Mediterranean region mapped from controlled-source and natural seismicity surveys, *Tectonophysics*, 692, 74–85, <https://doi.org/10.1016/j.tecto.2016.08.023>, 2016.
- Do Couto, D., Gumiaux, C., Augier, R., Le Bret, N., Folcher, N., Jouannic, G., Jolivet, L., Suc, J., and Gorini, C.: Tectonic inversion of an asymmetric graben: Insights from a combined field and gravity survey in the Sorbas basin, *Tectonics*, 33, 1360–1385, <https://doi.org/10.1002/2013tc003458>, 2014.
- Duggen, S., Hoernle, K., Bogaard, P., van den Rüpke, L., and Morgan, J. P.: Deep roots of the Messinian salinity crisis, *Nature*, 422, 602–606, <https://doi.org/10.1038/nature01553>, 2003.
- Duggen, S., Hoernle, K., Bogaard, P., and van den Harris, C.: Magmatic evolution of the Alboran region: The role of subduction in forming the western Mediterranean and causing the Messinian Salinity Crisis, *Earth. Planet. Sc. Lett.*, 218, 91–108, [https://doi.org/10.1016/s0012-821x\(03\)00632-0](https://doi.org/10.1016/s0012-821x(03)00632-0), 2004.
- Duggen, S., Hoernle, K., Klügel, A., Geldmacher, J., Thirlwall, M., Hauff, F., Lowry, D., and Oates, N.: Geochemical zonation of the Miocene Alborán Basin volcanism (westernmost Mediterranean): geodynamic implications, *Contrib. Mineral. Petr.*, 156, 577, <https://doi.org/10.1007/s00410-008-0302-4>, 2008.
- Echeverría, A., Khazaradze, G., Asensio, E., Gárate, J., Dávila, J. M., and Suriñach, E.: Crustal deformation in eastern Betics from CuaTeNeo GPS network, *Tectonophysics*, 608, 600–612, <https://doi.org/10.1016/j.tecto.2013.08.020>, 2013.
- Ercilla, G., Galindo-Zaldivar, J., Estrada, F., Valencia, J., Juan, C., Casas, D., Alonso, B., Comas, M. C., Tendero-Salmerón, V., Casalbore, D., Azpiroz-Zabala, M., Bárcenas, P., Cerami-cola, S., Chiocci, F. L., Idárraga-García, J., López-González, N., Mata, P., Palomino, D., Rodríguez-García, J. A., Teixeira, M., Nespereira, J., Vázquez, J. T., and Yenes, M.: Understanding the complex geomorphology of a deep sea area affected by continental tectonic indentation: The case of the Gulf of Vera (Western Mediterranean), *Geomorphology*, 402, 108126, <https://doi.org/10.1016/j.geomorph.2022.108126>, 2022.
- Faccenna, C., Becker, T. W., Auer, L., Billi, A., Boschi, L., Brun, J. P., Capitanio, F. A., Funicello, F., Horvath, F., Jolivet, L., Piro-mallo, C., Royden, L., Rossetti, F., and Serpelloni, E.: Mantle dynamics in the Mediterranean, *Rev. Geophys.*, 52, 283–332, <https://doi.org/10.1002/2013rg000444>, 2014.
- Fadil, A., Vernant, P., McClusky, S., Reilinger, R., Gomez, F., Sari, D. B., Mourabit, T., Feigl, K., and Barazangi, M.: Active tectonics of the western Mediterranean: Geodetic evidence for rollback of a delaminated subcontinental lithospheric slab beneath the Rif Mountains, Morocco, *Geology*, 34, 529–532, <https://doi.org/10.1130/g22291.1>, 2006.
- Fortuin, A. R. and Krijgsman, W.: The Messinian of the Nijar Basin (SE Spain): sedimentation, depositional environments and paleogeographic evolution, *Sediment. Geol.*, 160, 213–242, [https://doi.org/10.1016/s0037-0738\(02\)00377-9](https://doi.org/10.1016/s0037-0738(02)00377-9), 2003.
- Fossen, H., Teyssier, C., and Whitney, D.L.: Transtensional folding, *J. Struct. Geol.*, 56, 89–102, <https://doi.org/10.1016/j.jsg.2013.09.004>, 2013.
- Fossen, H. and Tikoff, B.: Extended models of transpression and transtension, and application to tectonic settings, *Geol. Soc. London Spec. Pub.*, 135, 15–33, <https://doi.org/10.1144/gsl.sp.1998.135.01.02>, 1998.
- Galindo-Zaldivar, J., Gonzalez-Lodeiro, F., and Jabaloy, A.: Progressive extensional shear structures in a detachment contact in the Western Sierra Nevada (Betic Cordilleras, Spain), *Geodin. Acta*, 3, 73–85, <https://doi.org/10.1080/09853111.1989.11105175>, 2015.
- Galindo-Zaldivar, J., Gil, A. J., Borque, M. J., González-Lodeiro, F., Jabaloy, A., Marin-Lechado, C., Ruano, P., and Sanz de Galdeano, C.: Active faulting in the internal zones of the central Betic Cordilleras (SE, Spain), *J. Geodyn.*, 36, 239–250, [https://doi.org/10.1016/s0264-3707\(03\)00049-8](https://doi.org/10.1016/s0264-3707(03)00049-8), 2003.

- Gallais, F., Graindorge, D., Gutscher, M.-A., and Klaeschen, D.: Propagation of a lithospheric tear fault (STEP) through the western boundary of the Calabrian accretionary wedge offshore eastern Sicily (Southern Italy), *Tectonophysics*, 602, 141–152, <https://doi.org/10.1016/j.tecto.2012.12.026>, 2013.
- García-Castellanos, D. and Villaseñor, A.: Messinian salinity crisis regulated by competing tectonics and erosion at the Gibraltar arc, *Nature*, 480, 359–363, <https://doi.org/10.1038/nature10651>, 2012.
- García-Dueñas, V., Banda, E., Torné, M., Córdoba, D., and ESCI-Béticas Working Group: A deep seismic reflection survey across the Betic Chain (southern Spain): first results, *Tectonophysics*, 232, 77–89, [https://doi.org/10.1016/0040-1951\(94\)90077-9](https://doi.org/10.1016/0040-1951(94)90077-9), 1994.
- Giaconia, F., Booth-Rea, G., Martínez-Martínez, J. M., Azañón, J. M., Pérez-Peña, J. V., Pérez-Romero, J., and Villegas, I.: Geomorphic evidence of active tectonics in the Sierra Alhamilla (eastern Betics, SE Spain), *Geomorphology*, 145, 90–10, <https://doi.org/10.1016/j.geomorph.2011.12.043>, 2012.
- Giaconia, F., Booth-Rea, G., Martínez-Martínez, J. M., Azañón, J. M., Pérez-Romero, J., and Villegas, I.: Mountain front migration and drainage captures related to fault segment linkage and growth: The Polopos transpressive fault zone (southeastern Betics, SE Spain), *J. Struct. Geol.*, 46, 76–91, <https://doi.org/10.1016/j.jsg.2012.10.005>, 2013.
- Giaconia, F., Booth-Rea, G., Martínez-Martínez, J. M., Azañón, J. M., Storti, F., and Artoni, A.: Heterogeneous extension and the role of transfer faults in the development of the southeastern Betic basins (SE Spain), *Tectonics*, 33, 2467–2489, <https://doi.org/10.1002/2014tc003681>, 2014.
- Giaconia, F., Booth-Rea, G., Ranero, C. R., Gràcia, E., Bartolome, R., Calahorrano, A., Iacono, C.L., Vendrell, M. G., Cameselle, A. L., Costa, S., Gómez de la Peña, L., Martínez-Lorient, S., Perea, H., and Viñas, M.: Compressional tectonic inversion of the Algero-Balearic basin: Latest Miocene to present oblique convergence at the Palomares margin (Western Mediterranean): Tectonic Inversion of Palomares Margin, *Tectonics*, 34, 1516–1543, <https://doi.org/10.1002/2015tc003861>, 2015.
- Gomez-Pugnaire, M. T. and Fernandez-Soler, J. M.: High-pressure metamorphism in metabasites from the Betic Cordilleras (S.E. Spain) and its evolution during the Alpine orogeny, *Contrib. Mineral. Petr.*, 95, 231–244, <https://doi.org/10.1007/bf00381273>, 1987.
- Gómez de la Peña, L., Grevemeyer, I., Kopp, H., Díaz, J., Gallart, J., Booth-Rea, G., Gràcia, E., and Ranero, C. R.: The Lithospheric Structure of the Gibraltar Arc System From Wide-Angle Seismic Data, *J. Geophys. Res.-Solid Earth*, 125, e2020JB019854, <https://doi.org/10.1029/2020jb019854>, 2020a.
- Gómez de la Peña, L., Ranero, C. R., and Gràcia, E.: The Crustal Domains of the Alboran Basin (Western Mediterranean), *Tectonics*, 37, 3352–3377, <https://doi.org/10.1029/2017tc004946>, 2018.
- Gómez de la Peña, L., Ranero, C. R., Gràcia, E., and Booth-Rea, G.: The evolution of the westernmost Mediterranean basins, *Earth Sci. Rev.*, 214, 103445, <https://doi.org/10.1016/j.earscirev.2020.103445>, 2020b.
- Gonzalez-Castillo, L., Galindo-Zaldivar, J., Lacy, M. C. de, Borque, M. J., Martínez-Moreno, F. J., García-Armenteros, J. A., and Gil, A. J.: Active rollback in the Gibraltar Arc: Evidences from CGPS data in the western Betic Cordillera, *Tectonophysics*, 663, 310–321, <https://doi.org/10.1016/j.tecto.2015.03.010>, 2015.
- Govers, R. and Wortel, M. J. R.: Lithosphere tearing at STEP faults: response to edges of subduction zones, *Earth Planet. Sc. Lett.*, 236, 505–523, <https://doi.org/10.1016/j.epsl.2005.03.022>, 2005.
- Haq, B., Gorini, C., Baur, J., Moneron, J., and Rubino, J.-L.: Deep Mediterranean's Messinian evaporite giant: How much salt?, *Global Planet. Change*, 184, 103052, <https://doi.org/10.1016/j.gloplacha.2019.103052>, 2020.
- Haughton, P. D. W.: Evolving turbidite systems on a deforming basin floor, Tabernas, SE Spain, *Sedimentology*, 47, 497–518, <https://doi.org/10.1046/j.1365-3091.2000.00293.x>, 2000.
- Haughton, P. D. W.: Deposits of deflected and ponded turbidity currents, Sorbas Basin, Southeast Spain, *J. Sediment. Res.*, 64, 233–246, <https://doi.org/10.1306/d4267d6b-2b26-11d7-8648000102c1865d>, 1994.
- Heit, B., de Mancilla, F. L., Yuan, X., Morales, J., Stich, D., Martín, R., and Molina-Aguilera, A.: Tearing of the mantle lithosphere along the intermediate-depth seismicity zone beneath the Gibraltar Arc: The onset of lithospheric delamination, *Geophys. Res. Lett.*, 44, 4027–4035, <https://doi.org/10.1002/2017gl073358>, 2017.
- Hodgson, D. M. and Haughton, P. D. W.: Impact of syn-depositional faulting on gravity current behaviour and deep-water stratigraphy: Tabernas-Sorbas Basin, SE Spain, *Geol. Soc. London Spec. Pub.*, 222, 135–158, <https://doi.org/10.1144/gsl.sp.2004.222.01.08>, 2004.
- Jabaloy-Sánchez, A., Talavera, C., Rodríguez-Peces, M. J., Vázquez-Vílchez, M., and Evans, N. J.: U-Pb geochronology of detrital and igneous zircon grains from the Águilas Arc in the Internal Betics (SE Spain): Implications for Carboniferous-Permian paleogeography of Pangea, *Gondwana Res.*, 90, 135–158, <https://doi.org/10.1016/j.gr.2020.10.013>, 2021.
- Janowski, M., Loget, N., Gautheron, C., Barbarand, J., Bellahsen, N., Driessche, J. V. den Babault, J., and Meyer, B.: Neogene exhumation and relief evolution in the eastern Betics (SE Spain): Insights from the Sierra de Gador, *Terra Nova*, 29, 91–97, <https://doi.org/10.1111/ter.12252>, 2017.
- Johnson, C., Harbury, N., and Hurford, A. J.: The role of extension in the Miocene denudation of the Nevado-Filábride Complex, Betic Cordillera (SE Spain), *Tectonics*, 16, 189–204, <https://doi.org/10.1029/96tc03289>, 1997.
- Jolivet, L., Baudin, T., Calassou, S., Chevrot, S., Ford, M., Is-sautier, B., Lasseur, E., Masini, E., Manatschal, G., Mouthereau, F., Thinon, I., and Vidal, O.: Geodynamic evolution of a wide plate boundary in the Western Mediterranean, near-field versus far-field interactions, *Bsgf – Earth Sci. Bull.*, 192, 48, <https://doi.org/10.1051/bsgf/2021043>, 2021a.
- Jolivet, L. and Faccenna, C.: Mediterranean extension and the Africa-Eurasia collision, *Tectonics*, 19, 1095–1106, <https://doi.org/10.1029/2000tc900018>, 2000.
- Jolivet, L., Menant, A., Roche, V., Le Pourhiet, L., Mail-lard, A., Augier, R., Couto, D. D., Gorini, C., Thinon, I., and Canva, A.: Transfer zones in Mediterranean back-arc regions and tear faults, *Bsgf – Earth Sci. Bulletin*, 192, 11, <https://doi.org/10.1051/bsgf/2021006>, 2021b.
- Jourdon, A., Kergaravat, C., Duclaux, G., and Huguén, C.: Looking beyond kinematics: 3D thermo-mechanical modelling reveals

- the dynamics of transform margins, *Sol. Earth*, 12, 1211–1232, <https://doi.org/10.5194/se-12-1211-2021>, 2021.
- Juan, C., Ercilla, G., Javier Hernández-Molina, F., Estrada, F., Alonso, B., Casas, D., García, M., Farran, M., Llave, E., Palomino, D., Vázquez, J.-T., Medialdea, T., Gorini, C., D'Acremont, E., Moumni, B. E., and Ammar, A.: Seismic evidence of current-controlled sedimentation in the Alboran Sea during the Pliocene and Quaternary: Palaeoceanographic implications, *Mar. Geol.*, 378, 292–311, <https://doi.org/10.1016/j.margeo.2016.01.006>, 2016.
- Jurado, M. J. and Comas, M. C.: Well log interpretation and seismic character of the cenozoic sequence in the northern Alboran Sea, *Geo-Mar. Lett.*, 12, 129–136, <https://doi.org/10.1007/BF02084923>, 1992.
- Kleverlaan, K.: Neogene history of the Tabernas basin (SE Spain) and its Tortonian submarine fan development, *Geol. Mijnbouw*, 421–432, 1989.
- Kleverlaan, K.: Three distinctive feeder-lobe systems within one time slice of the Tortonian Tabernas fan, SE Spain, *Sedimentology*, 36, 25–45, <https://doi.org/10.1111/j.1365-3091.1989.tb00818.x>, 1989.
- Kleverlaan, K.: Gordo megabed: a possible seismite in a tortonian submarine fan, tabernas basin, province almeria, southeast spain, *Sediment Geol.*, 51, 165–180, [https://doi.org/10.1016/0037-0738\(87\)90047-9](https://doi.org/10.1016/0037-0738(87)90047-9), 1987.
- Koulali, A., Ouazar, D., Tahayt, A., King, R.W., Vernant, P., Reilinger, R.E., McClusky, S., Mourabit, T., Davila, J. M., and Amraoui, N.: New GPS constraints on active deformation along the Africa–Iberia plate boundary, *Earth Planet. Sc. Lett.*, 308, 211–217, <https://doi.org/10.1016/j.epsl.2011.05.048>, 2011.
- De Larouzière, F. D., Bolze, J., Bordet, P., Hernandez, J., Montenat, C., and Ott d'Estevou, P.: The Betic segment of the lithospheric Trans-Alboran shear zone during the Late Miocene, *Tectonophysics*, 152, 41–52, [https://doi.org/10.1016/0040-1951\(88\)90028-5](https://doi.org/10.1016/0040-1951(88)90028-5), 1988.
- Le Pourhiet, L., Huet, B., May, D. A., Labrousse, L., and Jolivet, L.: Kinematic interpretation of the 3D shapes of metamorphic core complexes: 3D shapes of MCCS, *Geochem. Geophys. Geosystems*, 13, Q09002, <https://doi.org/10.1029/2012gc004271>, 2012.
- Lonergan, L. and White, N.: Origin of the Betic-Rif mountain belt, *Tectonics*, 16, 504–522, <https://doi.org/10.1029/96tc03937>, 1997.
- Mancilla, F. de L., Booth-Rea, G., Stich, D., Pérez-Peña, J. V., Morales, J., Azañón, J. M., Martín, R., and Giaconia, F.: Slab rupture and delamination under the Betics and Rif constrained from receiver functions, *Tectonophysics*, 663, 225–237, <https://doi.org/10.1016/j.tecto.2015.06.028>, 2015a.
- Mancilla, F. de L., Heit, B., Morales, J., Yuan, X., Stich, D., Molina-Aguilera, A., Azañón, J. M., and Martín, R. A.: STEP fault in Central Betics, associated with lateral lithospheric tearing at the northern edge of the Gibraltar arc subduction system, *Earth Planet. Sc. Lett.*, 486, 32–40, <https://doi.org/10.1016/j.epsl.2018.01.008>, 2018.
- Mancilla, F. de L., Stich, D., Morales, J., Martín, R., Díaz, J., Pazos, A., Córdoba, D., Pulgar, J. A., Ibarra, P., Harnafi, M., and Gonzalez-Lodeiro, F.: Crustal thickness and images of the lithospheric discontinuities in the Gibraltar arc and surrounding areas, *Geophys. J. Int.*, 203, 1804–1820, <https://doi.org/10.1093/gji/ggv390>, 2015b.
- Martin, J. M., Braga, J. C., and Rivas, P.: Coral successions in Upper Tortonian reefs in SE Spain, *Lethaia*, 22, 271–286, <https://doi.org/10.1111/j.1502-3931.1989.tb01342.x>, 1989.
- Martín, J. M. and Braga, J. C.: Messinian events in the Sorbas Basin in southeastern Spain and their implications in the recent history of the Mediterranean, *Sediment Geol.*, 90, 257–268, [https://doi.org/10.1016/0037-0738\(94\)90042-6](https://doi.org/10.1016/0037-0738(94)90042-6), 1994.
- Martínez-García, P., Comas, M., Lonergan, L., and Watts, A. B.: From Extension to Shortening: Tectonic Inversion Distributed in Time and Space in the Alboran Sea, Western Mediterranean, *Tectonics*, 36, 2777–2805, <https://doi.org/10.1002/2017tc004489>, 2017.
- Martínez-García, P., Soto, J. I., and Comas, M.: Recent structures in the Alboran Ridge and Yusuf fault zones based on swath bathymetry and sub-bottom profiling: evidence of active tectonics, *Geo-Mar. Lett.*, 31, 19–36, <https://doi.org/10.1007/s00367-010-0212-0>, 2011.
- Martínez-Martínez, J. M. and Azañón, J. M.: Mode of extensional tectonics in the southeastern Betics (SE Spain): Implications for the tectonic evolution of the peri-Alborán orogenic system, *Tectonics*, 16, 205–225, <https://doi.org/10.1029/97tc00157>, 1997.
- Martínez-Martínez, J. M., Booth-Rea, G., Azañón, J. M., and Torcal, F.: Active transfer fault zone linking a segmented extensional system (Betics, southern Spain): Insight into heterogeneous extension driven by edge delamination, *Tectonophysics*, 422, 159–173, <https://doi.org/10.1016/j.tecto.2006.06.001>, 2006.
- Martínez-Martínez, J. M., Soto, J. I., and Balanyá, J. C.: Orthogonal folding of extensional detachments: Structure and origin of the Sierra Nevada elongated dome (Betics, SE Spain), *Tectonics*, 21, 1012, <https://doi.org/10.1029/2001tc001283>, 2002.
- Martínez-Martínez, J. M., Soto, J. I., and Balanyá, J. C.: Elongated domes in extended orogens: A mode of mountain uplift in the Betics (southeast Spain), in: *Special Paper 380: Gneiss Domes in Orogeny*, edited by: Whitney, D., Teyssier, C., and Siddoway, C. S., Geological Society of America, 243–265, <https://doi.org/10.1130/0-8137-2380-9.243>, 2004.
- Martínez-Martos, M., Galindo-Zaldívar, J., Martínez-Moreno, F. J., Calvo-Rayó, R., and Sanz de Galdeano, C.: Superposition of tectonic structures leading elongated intramontane basin: the Alhabia basin (Internal Zones, Betic Cordillera), *Int. J. Earth Sci.*, 106, 2461–2471, <https://doi.org/10.1007/s00531-016-1442-9>, 2017.
- Meighan, H. E., ten Brink, U., and Pulliam, J.: Slab tears and intermediate-depth seismicity: slab tears and intermediate seismicity, *Geophys. Res. Lett.*, 40, 4244–4248, <https://doi.org/10.1002/grl.50830>, 2013.
- Meijninger, B. M. L. and Vissers, R. L. M.: Miocene extensional basin development in the Betic Cordillera, SE Spain revealed through analysis of the Alhama de Murcia and Crevillente Faults: Miocene extensional basin development in the Betic Cordillera, *Basin Res.*, 18, 547–571, <https://doi.org/10.1111/j.1365-2117.2006.00308.x>, 2006.
- Montenat, C. and d'Estevou, P. O.: Geodynamics of the Eastern Betic late Neogene Basins. A Review, *Física de la Tierra*, 57–75, ISSN 0214-4557, 1992.
- Montenat, C. and d'Estevou, P. O.: The diversity of late Neogene sedimentary basins generated by wrench faulting in the eastern Betic Cordillera, SE Spain, *J. Petrol. Geol.*, 22, 61–80, <https://doi.org/10.1111/j.1747-5457.1999.tb00459.x>, 1999.

- Mora, M.: Tectonic and sedimentary analysis of the Huerca-Overa region, South East Spain, Betic Cordillera, PhD thesis, University of Oxford, 300 pp., <https://openaccess.library.uitm.edu.my/Record/ndltd-bl.uk-oai-ethos.bl.uk-336120> (last access: 1 December 2023), 1993.
- Moragues, L., Ruano, P., Azañón, J. M., Garrido, C. J., Hidas, K., and Booth-Rea, G.: Two Cenozoic Extensional Phases in Mallorca and Their Bearing on the Geodynamic Evolution of the Western Mediterranean, *Tectonics*, 40, e2021TC006868, <https://doi.org/10.1029/2021tc006868>, 2021.
- Mouthereau, F., Angrand, P., Jourdon, A., Ternois, S., Fillon, C., Calassou, S., Chevrot, S., Ford, M., Jolivet, L., Manatschal, G., Masini, E., Thion, I., Vidal, O., and Baudin, T.: Cenozoic mountain building and topographic evolution in Western Europe: impact of billions of years of lithosphere evolution and plate kinematics, *Bsgf – Earth Sci. Bull.*, 192, 56, <https://doi.org/10.1051/bsgf/2021040>, 2021.
- Mouthereau, F., Filleaudeau, P., Vacherat, A., Pik, R., Lacombe, O., Fellin, M.G., Castellort, S., Christophoul, F., and Masini, E.: Placing limits to shortening evolution in the Pyrenees: Role of margin architecture and implications for the Iberia/Europe convergence, *Tectonics*, 33, 2283–2314, <https://doi.org/10.1002/2014tc003663>, 2014.
- Neuharth, D., Brune, S., Glerum, A., Morley, C. K., Yuan, X., and Braun, J.: Flexural strike-slip basins, *Geology*, 50, 361–365, <https://doi.org/10.1130/g49351.1>, 2021.
- Nocquet, J.-M.: Present-day kinematics of the Mediterranean: A comprehensive overview of GPS results, *Tectonophysics*, 579, 220–242, <https://doi.org/10.1016/j.tecto.2012.03.037>, 2012.
- Okay, A.I., Tüysüz, O., and Kaya, Ş : From transpression to transtension: changes in morphology and structure around a bend on the North Anatolian Fault in the Marmara region, *Tectonophysics*, 391, 259–282, <https://doi.org/10.1016/j.tecto.2004.07.016>, 2004.
- Palano, M., González, P. J., and Fernández, J.: The Diffuse Plate boundary of Nubia and Iberia in the Western Mediterranean: Crustal deformation evidence for viscous coupling and fragmented lithosphere, *Earth Planet. Sci. Lett.*, 430, 439–447, <https://doi.org/10.1016/j.epsl.2015.08.040>, 2015.
- Palano, M., González P. J., and Fernández, J.: Strain and stress fields along the Gibraltar Orogenic Arc: Constraints on active geodynamics, *Gondwana Res.*, 23, 1071–1088, <https://doi.org/10.1016/j.gr.2012.05.021>, 2013.
- Palomeras, I., Thurner, S., Levander, A., Liu, K., Villaseñor, A., Carbonell, R., and Harnafi, M.: Finite-frequency Rayleigh wave tomography of the western Mediterranean: Mapping its lithospheric structure. *Geochem. Geophys. Geosyst.*, 15, 140–160, <https://doi.org/10.1002/2013gc004861>, 2014.
- Pedraza, A., Galindo-Zaldívar, J., Sanz de Galdeano, C., and López-Garrido, Á.C.: Fold and fault interactions during the development of an elongated narrow basin: The Almanzora Neogene-Quaternary Corridor (SE Betic Cordillera, Spain): fold and fault interactions, *Tectonics*, 26, TC6002, <https://doi.org/10.1029/2007tc002138>, 2007.
- Pedraza, A., Galindo-Zaldívar, J., Ruíz-Constán, A., Duque, C., Marín-Lechado, C., and Serrano, I.: Recent large fold nucleation in the upper crust: Insight from gravity, magnetic, magnetotelluric and seismicity data (Sierra de Los Filabres–Sierra de Las Estancias, Internal Zones, Betic Cordillera), *Tectonophysics*, 463, 145–160, <https://doi.org/10.1016/j.tecto.2008.09.037>, 2009.
- Pedraza, A., Galindo-Zaldívar, J., Tello, A., and Marín-Lechado, C.: Intramontane basin development related to contractional and extensional structure interaction at the termination of a major sinistral fault: The Huércal-Overa Basin (Eastern Betic Cordillera), *J. Geodyn.*, 49, 271–286, <https://doi.org/10.1016/j.jog.2010.01.008>, 2010.
- Pickering, K. T., Hodgson, D. M., Platzman, E., Clark, J. D., and Stephens, C.: A New Type of Bedform Produced by Backfilling Processes in a Submarine Channel, Late Miocene, Tabernas-Sorbas Basin, SE Spain, *J. Sediment Res.*, 71, 692–704, <https://doi.org/10.1306/2dc40960-0e47-11d7-8643000102c1865d>, 2001.
- Pindell, J. L. and Kennan, L.: Tectonic evolution of the Gulf of Mexico, Caribbean and northern South America in the mantle reference frame: an update, *Geol. Soc. London Special Publ.* 328, 1–55, <https://doi.org/10.1144/sp328.1>, 2009.
- Platt, J. P., Behr, W. M., Johanesen, K., and Williams, J. R.: The Betic-Rif Arc and Its Orogenic Hinterland: A Review, *Annu. Rev. Earth Planet. Sci.*, 41, 313–357, <https://doi.org/10.1146/annurev-earth-050212-123951>, 2013.
- Platt, J. P., Kelley, S. P., Carter, A., and Orozco, M.: Timing of tectonic events in the Alpujarride Complex, Betic Cordillera, southern Spain, *J. Geol. Soc. London*, 162, 451–462, <https://doi.org/10.1144/0016-764903-039>, 2005.
- Platt, J. P., Whitehouse, M. J., Kelley, S. P., Carter, A., and Hollick, L.: Simultaneous extensional exhumation across the Alboran Basin: Implications for the causes of late orogenic extension, *Geology*, 31, 251–254, [https://doi.org/10.1130/0091-7613\(2003\)031<0251:seeata>2.0.co;2](https://doi.org/10.1130/0091-7613(2003)031<0251:seeata>2.0.co;2), 2003.
- Platt, J. P., Anczkiewicz, R., Soto, J.-I., Kelley, S. P., and Thirlwall, M.: Early Miocene continental subduction and rapid exhumation in the western Mediterranean, *Geology*, 34, 981–984, <https://doi.org/10.1130/g22801a.1>, 2006.
- Platt, J. P. and Vissers, R. L. M.: Extensional collapse of thickened continental lithosphere: A working hypothesis for the Alboran Sea and Gibraltar arc, *Geology*, 17, 540–543, [https://doi.org/10.1130/0091-7613\(1989\)017<0540:ecotcl>2.3.co;2](https://doi.org/10.1130/0091-7613(1989)017<0540:ecotcl>2.3.co;2), 1989.
- Platt, J. P. and Whitehouse, M. J.: Early Miocene high-temperature metamorphism and rapid exhumation in the Betic Cordillera (Spain): evidence from U–Pb zircon ages, *Earth Planet. Sci. Lett.*, 171, 591–605, [https://doi.org/10.1016/S0012-821X\(99\)00176-4](https://doi.org/10.1016/S0012-821X(99)00176-4), 1999.
- Platzman, E. S.: Paleomagnetic rotations and the kinematics of the Gibraltar arc, *Geology*, 20, 311–314, [https://doi.org/10.1130/0091-7613\(1992\)020<0311:pratko>2.3.co;2](https://doi.org/10.1130/0091-7613(1992)020<0311:pratko>2.3.co;2), 1992.
- Poisson, A., Guezou, J. C., Ozturk, A., Inan, S., Temiz, H., Gürsöy, H., Kavak, K. S., and ÖZDEN, S.: Tectonic Setting and Evolution of the Sivas Basin, Central Anatolia, Turkey, *Int. Geol. Rev.*, 38, 838–853, <https://doi.org/10.1080/00206819709465366>, 1996.
- Poisson, A. M., Morel, J. L., Andrieux, J., Coulon, M., Wernli, R., and Guernet, C.: The origin and development of neogene basins in the SE Betic Cordillera (SE Spain): a case study of the Tabernas-Sorbas and Huerca Overa basins,

- J. Petrol. Geol., 22, 97–114, <https://doi.org/10.1111/j.1747-5457.1999.tb00461.x>, 1999.
- Pownall, J. M., Hall, R., and Watkinson, I. M.: Extreme extension across Seram and Ambon, eastern Indonesia: evidence for Banda slab rollback, *Sol. Earth*, 4, 277–314, <https://doi.org/10.5194/se-4-277-2013>, 2013.
- Rat, J., Mouthereau, F., Bricchau, S., Crémades, A., Bernet, M., Balvay, M., Ganne, J., Lahfid, A., and Gautheron, C.: Tectonothermal Evolution of the Cameros Basin: Implications for Tectonics of North Iberia, *Tectonics*, 38, 440–469, <https://doi.org/10.1029/2018tc005294>, 2019.
- Rat, J., Mouthereau, F., Bricchau, S., Vacherat, A., Fillon, C., and Gautheron, C.: Timing and distribution of exhumation in the Ebro basin reveal a plate-scale 10 Ma geodynamic event, *Global Planet. Change*, 18, 103973, <https://doi.org/10.1016/j.gloplacha.2022.103973>, 2022.
- Reicherter, K. and Hübscher, C.: Evidence for a seafloor rupture of the Carboneras Fault Zone (southern Spain): Relation to the 1522 Almería earthquake?, *J. Seismol.*, 11, 15–26, <https://doi.org/10.1007/s10950-006-9024-0>, 2006.
- Reinhardt, L. J., Dempster, T. J., Shroder, J. F., and Persano, C.: Tectonic denudation and topographic development in the Spanish Sierra Nevada, *Tectonics*, 26, TC3001, <https://doi.org/10.1029/2006tc001954>, 2007.
- Richards, J. P.: Postsubduction porphyry Cu-Au and epithermal Au deposits: Products of remelting of subduction-modified lithosphere, *Geology*, 37, 247–250, <https://doi.org/10.1130/g25451a.1>, 2009.
- Riding, R., Braga, J. C., Martin, J. M., and Sánchez-Almazo, I. M.: Mediterranean Messinian Salinity Crisis: constraints from a coeval marginal basin, Sorbas, southeastern Spain, *Mar. Geol.*, 146, 1–20, [https://doi.org/10.1016/s0025-3227\(97\)00136-9](https://doi.org/10.1016/s0025-3227(97)00136-9), 1998.
- Rodríguez-Fernández, J., Azor, A., and Azañón, J. M.: The Betic Intramontane Basins (SE Spain): Stratigraphy, Subsidence, and Tectonic History, in: *Tectonics of Sedimentary Basins: Recent Advances*, edited by: Busby, C. and Azor, A., Wiley-Blackwell, 461–479, <https://doi.org/10.1002/9781444347166.ch23>, 2012.
- Romagny, A., Jolivet, L., Menant, A., Bessi re, E., Maillard, A., Canva, A., Gorini, C., and Augier, R.: Detailed tectonic reconstructions of the Western Mediterranean region for the last 35 Ma, insights on driving mechanisms, *Bsgf – Earth Sci. Bull.*, 191, 37, <https://doi.org/10.1051/bsgf/2020040>, 2020.
- Rosenbaum, G., Lister, G. S., and Duboz, C.: Relative motions of Africa, Iberia and Europe during Alpine orogeny, *Tectonophysics*, 359, 117–129, [https://doi.org/10.1016/s0040-1951\(02\)00442-0](https://doi.org/10.1016/s0040-1951(02)00442-0), 2002.
- Sanz de Galdeano, C. and Vera, J. A.: Stratigraphic record and palaeogeographical context of the Neogene basins in the Betic Cordillera, Spain, *Basin Res.*, 4, 21–36, <https://doi.org/10.1111/j.1365-2117.1992.tb00040.x>, 1992.
- Sanz de Galdeano, C., Rodriguez-Fernandez, J., and Lopez-Garrido, A. C.: A strike-slip fault corridor within the Alpujarra Mountains (Betic Cordilleras, Spain), *Geol. Rundsch.*, 74, 641–655, <https://doi.org/10.1007/bf01821218>, 1985.
- Scotney, P., Burgess, R., and Rutter, E. H.: 40Ar/39Ar age of the Cabo de Gata volcanic series and displacements on the Carboneras fault zone, SE Spain, *J. Geol. Soc. London*, 157, 1003–1008, <https://doi.org/10.1144/jgs.157.5.1003>, 2000.
- Sosson, M., Morrillon, A.-C., Bourgeois, J., F raud, G., Poupeau, G., and Saint-Marc, P.: Late exhumation stages of the Alpujarride Complex (western Betic Cordilleras, Spain): new thermochronological and structural data on Los Reales and Ojen nappes, *Tectonophysics*, 285, 253–273, [https://doi.org/10.1016/s0040-1951\(97\)00274-6](https://doi.org/10.1016/s0040-1951(97)00274-6), 1998.
- Spakman, W. and Wortel, R.: A Tomographic View on Western Mediterranean Geodynamics, in: *The TRANSMED Atlas. The Mediterranean Region from Crust to Mantle*, edited by: Cavazza, W., Roure, F., Spakman, W., Stampfli, G. M., and Ziegler, P. A., Springer, Berlin, Heidelberg, 31–52, [https://doi.org/10.1007/978-3-642-18919-7\\_2](https://doi.org/10.1007/978-3-642-18919-7_2), 2004.
- Spakman, W., Chertova, M. V., Berg, A., and van Hinsbergen, D. J. J.: Puzzling features of western Mediterranean tectonics explained by slab dragging, *Nat. Geosci.*, 11, 211–216, <https://doi.org/10.1038/s41561-018-0066-z>, 2018.
- Stich, D., Serpelloni, E., Mancilla, F. de L., and Morales, J.: Kinematics of the Iberia–Maghreb plate contact from seismic moment tensors and GPS observations, *Tectonophysics*, 426, 295–317, <https://doi.org/10.1016/j.tecto.2006.08.004>, 2006.
- Tendero-Salmer n, V., Galindo-Zaldivar, J., d’Acremont, E., Catal n, M., Martos, Y.M., Ammar, A., and Ercilla, G.: New insights on the Alboran Sea basin extension and continental collision from magnetic anomalies related to magmatism (western Mediterranean), *Mar. Geol.*, 443, 106696, <https://doi.org/10.1016/j.margeo.2021.106696>, 2022.
- Teyssier, C. and Tikoff, B.: Strike-slip partitioned transpression of the San Andreas fault system: a lithospheric-scale approach, *Geol. Soc. London Spec. Pub.*, 135, 143–158, <https://doi.org/10.1144/gsl.sp.1998.135.01.10>, 1998.
- Vacherat, A., Mouthereau, F., Pik, R., Bellahsen, N., Gautheron, C., Bernet, M., Daudet, M., Balansa, J., Tibari, B., Jamme, R. P., and Radal, J.: Rift-to-collision transition recorded by tectonothermal evolution of the northern Pyrenees, *Tectonics*, 35, 907–933, <https://doi.org/10.1002/2015tc004016>, 2016.
- van Hinsbergen, D. J. J., Vissers, R. L. M., and Spakman, W.: Origin and consequences of western Mediterranean subduction, rollback, and slab segmentation, *Tectonics*, 33, 393–419, <https://doi.org/10.1002/2013tc003349>, 2014.
- V zquez, M., Jabaloy, A., Barbero, L., and Stuart, F. M.: Deciphering tectonic- and erosion-driven exhumation of the Nevado-Fil bride Complex (Betic Cordillera, Southern Spain) by low temperature thermochronology: Deciphering tectonic- and erosion-driven exhumation, *Terra Nova*, 23, 257–263, <https://doi.org/10.1111/j.1365-3121.2011.01007.x>, 2011.
- Verg s, J. and Fern ndez, M.: Tethys–Atlantic interaction along the Iberia–Africa plate boundary: The Betic–Rif orogenic system, *Tectonophysics*, 579, 144–172, <https://doi.org/10.1016/j.tecto.2012.08.032>, 2012.
- Vernant, P., Fadel, A., Mourabit, T., Ouazar, D., Koulali, A., Davila, J. M., Garate, J., McClusky, S., and Reilinger, R.: Geodetic constraints on active tectonics of the Western Mediterranean: Implications for the kinematics and dynamics of the Nubia–Eurasia plate boundary zone, *J. Geodyn.*, 49, 123–129, <https://doi.org/10.1016/j.jog.2009.10.007>, 2010.
- Villase nor, A., Chevrot, S., Harnafi, M., Gallart, J., Pazos, A., Serrano, I., C rdoba, D., Pulgar, J. A., and Ibarra, P.: Subduction and volcanism in the Iberia–North Africa collision zone from



- tomographic images of the upper mantle, *Tectonophysics*, 663, 238–249, <https://doi.org/10.1016/j.tecto.2015.08.042>, 2015.
- Waldner, M., Bellahsen, N., Mouthereau, F., Bernet, M., Pik, R., Rosenberg, C. L., and Balvay, M.: Central Pyrenees Mountain Building: Constraints From New LT Thermochronological Data From the Axial Zone, *Tectonics*, 40, e2020TC006614, <https://doi.org/10.1029/2020tc006614>, 2021.
- Weijermars, R., Roep, Th. B., van den Eeckhout, B., Postma, G., and Kleverlaan, K.: Uplift history of a Betic fold nappe inferred from Neogene-Quaternary sedimentation and tectonics (in the Sierra Alhamilla and Almeria, Sorbas and Tabernas Basins of the Betic Cordilleras, SE Spain), 397–411, *Geologie en Mijnbouw*, <https://drive.google.com/file/d/0B7j8bPm9Cse0SS11NUIWRmtmZE0/view?pli=1&resourcekey=0-AC79UAWcljTEJw6P7Y-CoA> (last access: 1 December 2023), 1985.
- Zeck, H. P., Monié, P., Villa, I. M., and Hansen, B. T.: Very high rates of cooling and uplift in the Alpine belt of the Betic Cordilleras, southern Spain, *Geology*, 20, 79, [https://doi.org/10.1130/0091-7613\(1992\)020<0079:vhroca>2.3.co;2](https://doi.org/10.1130/0091-7613(1992)020<0079:vhroca>2.3.co;2), 1992.